Syst. Biol. 75(1):135–155, 2026

https://doi.org/10.1093/sysbio/syaf055
Advance Access publication August 8, 2025

But the Clock, Tick-Tock: An Empirical Case Study Highlights the Preeminence of Relaxed Clock Models in Total-Evidence Dating

Nicolás Mongiardino Koch [1,2,3,*], Jeffrey R. Thompson[4,5], Rich Mooi[6], and Greg W. Rouse[1]

[1]*Scripps Institution of Oceanography, University of California San Diego, 9500 Gilman Drive, La Jolla, CA 92093, USA*
[2]*Department of Ecology and Evolutionary Biology, Princeton University, 11 Ivy Lane, Princeton, NJ 08544, USA*
[3]*Department of Biology, Colorado State University, 251 W Pitkin Street, Fort Collins, CO 80523, USA*
[4]*School of Biological Sciences, University of Southampton, Life Sciences Building (Building 85), Highfield Campus, Southampton SO17 1BJ, UK*
[5]*School of Ocean and Earth Science, University of Southampton, Waterfront Campus, European Way, Southampton, Hampshire SO14 3ZH, UK*
[6]*California Academy of Sciences, 55 Music Concourse Dr, San Francisco, CA 94118, USA*
[*]*Correspondence to be sent to: Department of Biology, Colorado State University, 251 W Pitkin Street, Fort Collins, CO 80523, USA.*
E-mail: n.mongiardinokoch@colostate.edu

Received 20 December 2024; reviews returned 7 July 2025; accepted 22 July 2025
Associate Editor: Seraina Klopfstein

Abstract.—Phylogenetic clock models translate inferred amounts of evolutionary change (calculated from either genotypes or phenotypes) into estimates of elapsed time, providing a mechanism for time scaling phylogenetic trees. Relaxed-clock models, which accommodate variation in evolutionary rates across branches, are one of the main components of Bayesian dating, yet their consequences for total-evidence phylogenetics have not been thoroughly explored. Here, we combine morphological, molecular (both transcriptomic and Sanger-sequenced), and stratigraphic data sets for all major lineages of echinoids (sea urchins, heart urchins, sand dollars). We then perform total-evidence dated inference under the fossilized birth–death prior, varying two analytical conditions: the choice between autocorrelated and uncorrelated relaxed clocks, which enforce (or not) evolutionary rate inheritance, and the ability to recover fossil terminals as direct ancestors. Our results highlight a previously unnoticed interaction between tree and clock models, with analyses implementing an autocorrelated clock failing to recover any direct ancestors. Nonetheless, even under conditions conducive to the placement of fossil terminals as ancestors, we find this type of relationship to be accommodated without any impact on either topology or node ages. On the other hand, tree topology, fossil placement, divergence times, and downstream macroevolutionary inferences (e.g., ancestral state reconstructions) were all strongly affected by the type of relaxed clock implemented. In regions of the tree where molecular rate variation is pervasive and morphological signal relatively uninformative, fossil tips seem to play little to no role in informing divergence times, and instead passively move in and out of clades depending on the ages imposed upon surrounding nodes by molecular data. Our results reveal the extent to which the phylogenetic and macroevolutionary conclusions of total-evidence dated analyses are contingent on the choice of relaxed-clock model, highlighting the need for either careful methodological validation or a thorough assessment of sensitivity. Our efforts continue to illuminate the echinoid tree of life, supporting the erection of the order Apatopygoida to include three living species last sharing a common ancestor with other extant lineages around the time of the Jurassic–Cretaceous boundary. Furthermore, they also illustrate how the phylogenetic placement of extinct clades hinges upon the modeling of molecular data, evidencing the extent to which the fossil record remains subservient to phylogenomics. [Echinoidea; fossilized birth–death; relaxed clocks; time calibration; tip dating; total evidence.]

A central tenet of evolutionary biology is that closely related species are more similar to each other than distantly related ones, an observation widely accepted by early naturalists whose generative mechanism was formalized by Darwin in the form of his theory of descent with modification (Darwin 1859). With the progression of time, similarities inherited from common ancestors become eroded as lineages experience independent evolutionary processes; those surviving constitute the data used to infer their phylogenetic relationships (Cracraft and Donoghue 2004; Maddison et al. 2007). Although some degree of proportionality between time and amount of change was rapidly accepted, its converse, that is, the use of observed differences to date divergences, was only first proposed by Zuckerkandl and Pauling (1962). The "molecular evolutionary clock" (Zuckerkandl and Pauling 1965), as it later became known, posited that the constancy of substitution rates among lineages and through time, coupled with paleontological calibrations, could be used to infer divergence times from amounts of change in molecular sequences. One of the direct results of this development was the ability to impart a geologic timescale to phylogenetic trees (Morgan 1998).

Early attempts to derive evolutionary timescales were limited in numerous ways: They made use of a fixed topology, resulting in overconfidence of divergence times due to a lack of propagation of topological uncertainty; they enforced a strict clock, making the unrealistic assumption of a total absence of rate variation; and they took the paleontological record at face value, directly applying fossil ages to internal nodes when these

can only provide partial information to date cladogenetic events. These limitations have since been superseded by methods of simultaneous Bayesian inference that rely on relaxed clocks and implement prior calibration densities (Sanderson 1997; Rambaut and Bromham 1998; Thorne et al. 1998; Yoder and Yang 2000; Benton and Ayala 2003; Graur and Martin 2004; Hedges and Kumar 2004; Drummond et al. 2006; Yang and Rannala 2006; Ho and Phillips 2009).

Although absent from their original formulation, molecular clocks were soon interpreted as an expected outcome of the predominant neutrality of molecular evolution (Kimura 1969). From this perspective, there seemed to be no room for morphological traits—whose evolution is primarily adaptive (Rieseberg et al. 2002; Ho et al. 2017)—to contribute to the inference of evolutionary timescales, even though such potential had been originally recognized (Mayr 1963; Simpson 1965). However, molecular clocks soon lost their preeminence in the neutralist-selectionist debates and became recognized instead as an emergent property of evolving biological systems, one whose usefulness remained even if it behaved only as an approximate, and often non-neutral, clock (Zuckerkandl 1987; Bromham and Penny 2003; Kumar 2005; Ho 2020). Soon after the adoption of statistical models of morphological evolution (Lewis 2001; Lee and Worthy 2012; Wright and Hillis 2014), researchers began inferring time-scaled trees (or chronograms) using morphological clocks, either on their own (Beck and Lee 2014; Lee et al. 2014) or alongside molecular ones (Pyron 2011; Ronquist et al. 2012a; Lee 2016).

The ability to infer chronograms that include extinct terminals revolutionized the fields of systematics, paleobiology, and macroevolution (Lee and Palci 2015; Hunt and Slater 2016; López-Antoñanzas et al. 2022). Node calibrations can only incorporate a small fraction of the fossil record's temporal information, whereas a precise phylogenetic placement for fossils that are fragmentary or display intermediate morphologies can be hard to ascertain—caveats that are alleviated by the joint inference of topology and node ages using dated tips (i.e., "tip dating"; Ronquist et al. 2012a; O'Reilly et al. 2015). The development of the fossilized birth–death (FBD) process (Heath et al. 2014), which models the history of diversification underlying the tree structure, further provided a natural and mechanistic framework to combine extant and fossil taxa and also allowed for the inference of ancestor-descendant relationships among sampled terminals (Gavryushkina et al. 2017; Pett and Heath 2020; Wright et al. 2022). As genetic data became widely available, the inference of chronograms using a combination of molecular, morphological, and stratigraphic information, and sampling across both living and extinct lineages—known as total-evidence dating (TED; Ronquist et al. 2012a; Zhang et al. 2016)—became the gold standard for the inference of phylogenetic, biogeographic, and macroevolutionary history (Arcila et al. 2015; Lee 2016; Ronquist et al. 2016; Gavryushkina et al. 2017; Pyron 2017; Lee and Yates 2018; Simões et al. 2020b; May et al. 2021; Mongiardino Koch and Thompson 2021; Troyer et al. 2022; Faurby et al. 2024; Tejada et al. 2024).

TED relies on a tripartite modeling framework (Warnock and Wright 2020) that includes a model of diversification (or tree prior, typically an FBD process), a model of trait evolution, and a (usually relaxed) clock model. Recent years have seen extensive efforts devoted to test the first of these (Matschiner 2019; Luo et al. 2020; O'Reilly and Donoghue 2020; May et al. 2021; Barido-Sottani et al. 2023; Simões et al. 2023b; Zhang et al. 2023), as well as to characterize the behavior of models of morphological change (Wright et al. 2016; Klopfstein et al. 2019; Rosa et al. 2019; Khakurel et al. 2024; Mulvey et al. 2025; Wright and Wynd 2024). The impact of implementing alternative relaxed-clock models within a TED framework has received comparatively less attention. For example, the choice between autocorrelated and uncorrelated clock models, which differ on whether they assume or not, respectively, the existence of evolutionary rate inheritance, can dramatically impact timescales inferred by node dating molecular trees (Lartillot et al. 2016; Dos Reis et al. 2018; Mongiardino Koch and Milla Carmona 2024). This is likely to be especially important when working with sparse taxonomic samples of ancient clades, in which case the limited amount of data is likely to render dating particularly contingent upon modeling assumptions. How alternative relaxed clocks affect key aspects of TED inference, such as fossil placement, recovery of ancestral-descendant relationships among sampled taxa, and rates of morphological change, remains relatively unexplored.

Echinoderms represent an ideal empirical system for phylogenetically grounded studies of macroevolution and paleobiology (e.g., Hopkins and Smith 2015; Wright 2017; Deline et al. 2020; Lam et al. 2021; Mongiardino Koch 2021a; Wright et al. 2021; Thuy et al. 2022). Their complex skeleton, composed of multiple elements of durable calcitic stereom (in some lineages forming tightly interlocked structures, such as the echinoid test and the crinoid calyx), endows them with both a highly informative morphology and a remarkable preservation potential. The resulting wealth of echinoderm paleontological data can be readily integrated with information for extant lineages, producing robust morphological phylogenies extending back to Mesozoic or Paleozoic times (Kroh and Smith 2010; Thuy and Stöhr 2016; Rahman et al. 2019; Souto et al. 2019; Fau and Villier 2023; Saulsbury and Baumiller 2023). Nonetheless, only one echinoderm TED analysis has been performed to date—the echinoid (sea urchin) phylogeny of Mongiardino Koch and Thompson (2021).

Our goal here is to revisit and build upon the aforementioned study, leveraging state-of-the-art methodologies with extensive morphological, molecular (both transcriptomic and Sanger-sequenced), and stratigraphic data sets to infer the phylogenetic relationships and divergence times of all major living and extinct

lineages of Echinoidea. Furthermore, we explore the effects induced by the choice of different parametric conditions, including alternative clock models (uncorrelated vs. autocorrelated relaxed clocks) and tree priors (possibility of direct ancestry). Rather than finding an optimal set of modeling conditions, we explore the sensitivity of results to methodological choices, allowing us to evaluate their interactions, and highlighting the extent to which TED phylogenies and downstream macroevolutionary conclusions are impacted by modeling assumptions.

Materials and Methods

Data Set Construction

Morphological data.— The morphological matrix for this study is taken from the seminal work of Kroh and Smith (2010), which scored a diversified sample of terminals by targeting all family/subfamily level clades of post-Paleozoic echinoids. These taxa are currently classified at various taxonomic ranks, so we redefined the operational taxonomic units (OTUs) of this data set as the most inclusive echinoid clades in the World Register of Marine Species (WoRMS Editorial Board 2024), containing a single coded species each. For the most part, these corresponded to either families, subfamilies, or tribes, although a handful of OTUs represent genus-level clades. Regardless of the taxonomic rank at which these terminals are currently recognized, they still represent a maximally diversified sample of echinoid clades from both taxonomic and morphological perspectives. In the original study, six families were excluded due to their incomplete or aberrant morphology, whereas a further five were removed after analyses to improve resolution. Here, we reincorporate the latter in the hopes that their placement will be more stable in a TED framework. We further added *Lissodiadema lorioli* (Mortensen 1903) as a terminal given that Lissodiadematidae is currently recognized at the family level (as the sister group of Diadematidae; WoRMS Editorial Board 2024), which further prompted a revision of the scorings of *Diadema antillarum* (Philippi 1845). We also removed *Poriocidaris purpurata* (Thomson 1872), a taxon now placed within the genus *Histocidaris*, leaving Histocidaridae represented only by *H. elegans* (Agassiz 1879). Readers are cautioned that conclusions drawn in this study might be affected by such a sparse taxon sampling.

Following Hopkins and Smith (2015) and Mongiardino Koch and Thompson (2021), we removed three characters from the original matrix and edited five others to correct errors. The final matrix, available in the Supplementary Material, contained 169 terminals and included the late stem-group Archaeocidaridae as the single morphological outgroup (Thompson et al. 2020). A total of 303 morphological characters were employed, describing traits that are variable and diagnostic at the targeted taxonomic levels, yet invariant below them (i.e., among both the extant and extinct diversity contained within OTUs). This peculiarity of the matrix makes it possible to combine morphological scorings with molecular data obtained from different species—as long as there is no reason to doubt the two are drawn from a clade that does not include any other sampled taxon—an avenue previously exploited in Mongiardino Koch and Thompson (2021). As in Kroh and Smith (2010), 16 characters were treated as ordered. Missing/inapplicable data represented 17.7% of cells for extant terminals and 29.5% for fossils.

Molecular data.— We incorporated two molecular data sets: the phylogenomic matrix of Mongiardino Koch et al. (2022) and a newly gathered data set of Sanger-sequenced loci. The first was downsampled by retaining loci with an occupancy above 80% and then sorted using *genesortR* (Mongiardino Koch 2021b) in the R statistical environment (R Core Team 2024). We retained the 25 loci exhibiting the highest phylogenetic usefulness, defined using a multivariate approach that simultaneously targets high phylogenetic signal and low evidence of systematic biases (Mongiardino Koch 2021b; Mongiardino Koch and Thompson 2021). Whenever multiple terminals were available for a given OTU, the highest occupancy one was kept. The sea cucumber *Holothuria forskali* (Delle Chiaje 1824) was used as the single molecular outgroup. Empty positions in the alignments left behind after taxon deletion were removed. The final data set included 5017 amino acids, spanning 33 of the 77 extant echinoid OTUs (see Fig. 1). The maximum likelihood (ML) topology for this data set is shown in Supplementary Figure S1, showing a high degree of concordance with the phylogenies of Mongiardino Koch et al. (2022) despite including less than 2% of the loci. Inference details can be found in the Supplementary Materials.

To build a new data set incorporating publicly available Sanger-sequenced data, all sequences of taxonomically non-redundant echinoids were downloaded from GenBank in September 2021. This database was clustered into homologous loci using the approach described in Yang and Smith (2014), as implemented by Picciani et al. (2018). Briefly, we performed an all-by-all BLAST search (Camacho et al. 2009) to obtain pairwise similarity scores, and obtained sequence clusters using MCL v.14-137 (Van Dongen 2000), imposing a degree of sequence overlap above 50% and using an inflation index of 1.0. The taxonomic breadth of the resulting clusters was explored by automatically assigning sequences to the higher-level OTUs of the morphological matrix. This relied on the R script *match_seq_to_taxonomy.R* (available on the Dryad repository), which uses as input a list of targeted OTUs and a taxonomic hierarchy. The latter was generated by web scraping the WoRMS repository using *deWoRMR* (https://github.com/mongiardino/deWoRMR), producing a table of all clade names to which each echinoid species

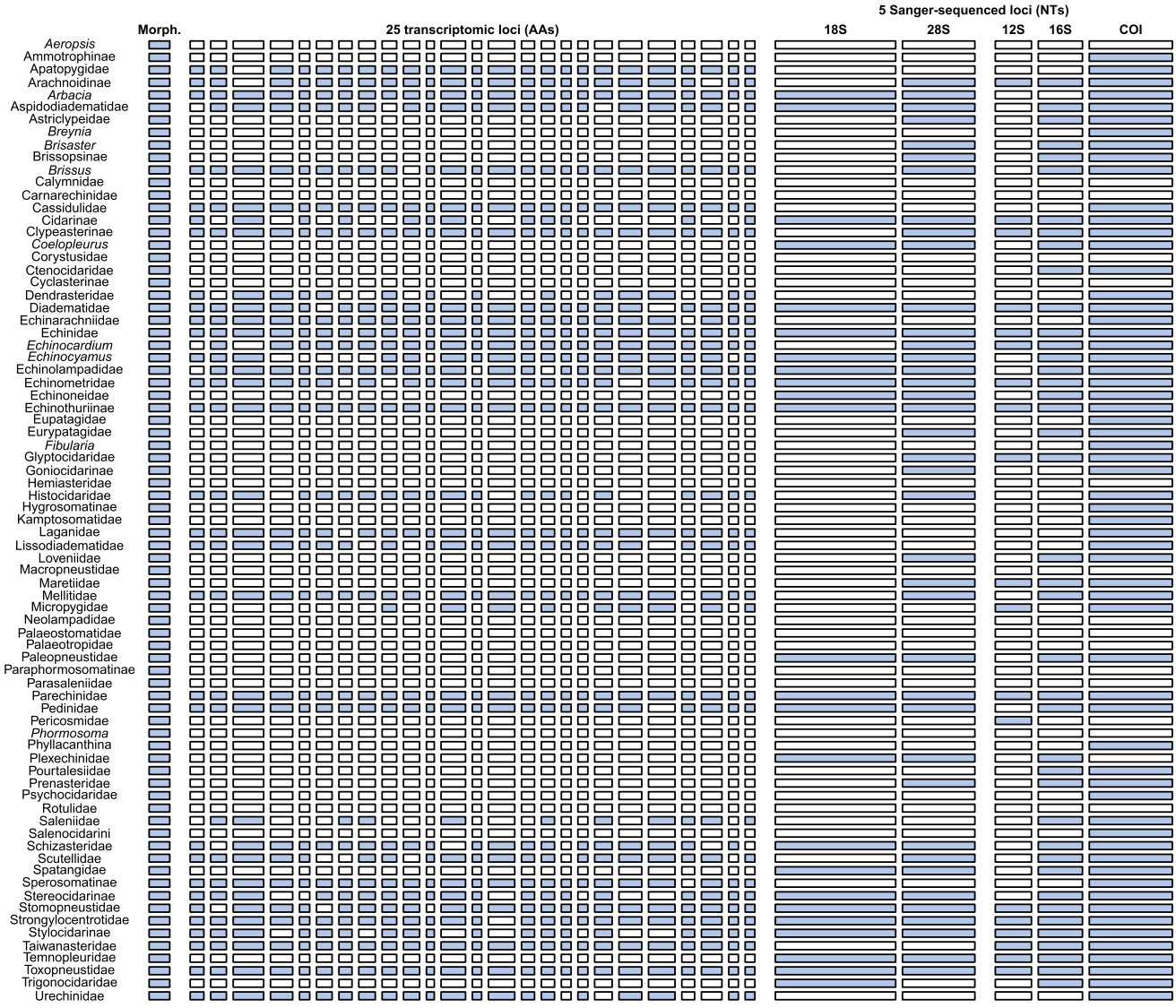

FIGURE 1. Total-evidence data set of major echinoid clades assembled for this study. Columns represent the different matrices combined, including (from left to right) morphology, 25 transcriptomic loci coded as amino acids, and 5 Sanger-sequenced loci coded as nucleotides (nuclear: 18S rRNA and 28S rRNA, mitochondrial: 12S rRNA, 16S rRNA, and COI). Bar widths are scaled to the number of characters within each; blue bars represent partitions with data. Rows represent each of the 77 extant echinoid OTUs. The complete data set further included the extant sea cucumber *Holothuria forskali* (coded only for molecular partitions) and 92 extinct echinoid clades (coded only for morphology). Information about each sequence (species, GenBank/SRA accession number) can be found in Supplementary Table S1.

is assigned (scraped in July 2021). The fraction of OTUs represented within each cluster was tallied, and those containing data for less than 10% were discarded. Remaining clusters were further reduced to one sequence per OTU by retaining the species taxonomically closest to those included in the other data sets (i.e., morphological or phylogenomic, with priority given to the latter). If more than one sequence was deemed equally close taxonomically, the longest was retained. Although this approach sought to reduce the degree of chimerism—that is, the extent to which molecular data from multiple species were combined into a single terminal—chimeric terminals are nonetheless common in our final data set (see below). Furthermore, the success of this approach in generating useful molecular data sets depends on the correct identification of publicly available sequences on GenBank. Although the impact of incorrect identifications might be diminished by the use of higher-level OTUs, this remains a key assumption that was not tested. Data handling relied on R packages *ape* (Paradis and Schliep 2019), *phangorn* (Schliep 2011), and *tidyverse* (Wickham et al. 2019).

Nine clusters remained, including sequences of the nuclear 18S and 28S ribosomal RNA (rRNA; one and

three clusters, respectively), mitochondrial 12S and 16S rRNA (one cluster each), cytochrome oxidase I (COI; two clusters), as well as a cluster containing complete mitogenomes. Preliminary alignments using MAFFT v.7.525 (Katoh and Standley 2013) revealed the multiple clusters of 28S and COI to be composed of one or more small fragments entirely nested within a larger one; thus, the corresponding clusters were merged, and the longest sequence per OTU was selected. Existing COI data were complemented with newly generated data for nine OTUs (highlighted in Supplementary Table S1), representing major echinoid lineages that lacked publicly available data. COI was amplified using primers and PCR settings detailed in Arndt et al. (1996); products were purified with ExoSAP-IT (USB Corporation, OH, USA) and sequenced by Eurofins Genomics (Louisville, KY, USA). Forward and reverse sequences were de novo assembled on Geneious Prime 2023.2.2 (http://www.geneious.com) under default settings. Consensus reads were generated after removing base pairs of poor quality and manually resolving most ambiguities. One extra COI sequence was mined from the transcriptome of *Echinarachnius parma* using the top BLAST hit against the COI sequence of the closely related *Dendraster excentricus*. These sequences are deposited under GenBank accession numbers PQ619100–PQ619108.

Finally, mitochondrial loci (12S, 16S, and COI) were concatenated respecting the conserved echinoid mitochondrial gene order (Perseke et al. 2010), combined with complete mitogenomes, and aligned using the E-INS-i algorithm. Both nuclear rRNA data sets were separately aligned with the L-INS-i algorithm. Gappy columns were deleted using trimAl v.1.5.0 (Capella-Gutiérrez et al. 2009), using a gap threshold of 0.24 for mitogenomes and 0.60 for nuclear rRNAs. Although initial efforts sought to use the entire mitogenome alignment, run times proved exceedingly long. Coupled with the fact that mitogenome occupancy was low (present in only 14 terminals), a decision was made to focus instead on the three genes with the highest occupancy (i.e., 12S, 16S, and COI), which were excised from the mitogenome alignment and used instead. The ML topology obtained from the concatenated analysis of these five Sanger-sequenced loci is shown in Supplementary Figure S2. The discrepancy between this tree and our current understanding of echinoid relationships is substantial, yet not unlike that of previous attempts relying on small numbers of markers (e.g., Littlewood and Smith 1995; Bronstein et al. 2018).

The five Sanger-sequenced loci obtained with this approach were incorporated into the final data set—represented in Figure 1—as 5229 nucleotide positions. The final extent of this merged molecular data set was 11,146 positions (with a 53–47% split between amino acids and nucleotides, respectively) and 60 terminals. These included 20 genus-level chimeras (i.e., combining data for multiple species within the same genus) and 10 family-level chimeras (i.e., combining data for species within different genera). Partitioned ML inference of this data set shows that this approach succeeded in extending the occupancy of the transcriptomic data while maintaining relatively low levels of phylogenetic error (Supplementary Fig. S3). All molecular data employed are identified in Supplementary Table S1, along with further justifications regarding the use of chimeric terminals.

Stratigraphic data.— OTUs with any amount of molecular data were considered extant, even when the species used for morphological coding was a fossil. For the remaining 95 OTUs, fossil ages were obtained from the primary literature and used as tip dates in the analysis. Additionally, 11 node dates were compiled from previous paleontological or phylogenetic studies (Smith et al. 2006; Thompson et al. 2017, 2019; Erkenbrack and Thompson 2019; Mongiardino Koch and Thompson 2021; Mongiardino Koch et al. 2022) and enforced for well-established monophyletic clades. All stratigraphic information is detailed in Supplementary Tables S2 (tip dates) and S3 (node dates).

Total-Evidence Dated Inference

Models of character evolution.— Optimal modeling and partitioning of each data type (morphology, amino acid, and nucleotide) was determined using ModelFinder (Kalyaanamoorthy et al. 2017) as implemented in IQ-TREE v.2.1.3 (Minh et al. 2020). Partition merging was activated (Chernomor et al. 2016), and best-fit models were selected based on Bayesian information criterion (BIC) scores. Only models implemented in MrBayes v.3.2.7a (Ronquist et al. 2012b) were considered.

For morphological data, model space was circumscribed to the Mk_v model (Lewis 2001) with and without gamma-distributed rate variation; partitioning schemes explored were (1) unpartitioned, (2) by number of states, (3) by anatomical region, (4) similarity-based, and (5) homoplasy-based. Anatomical partitioning followed the regions defined by Kroh and Smith (2010). Similarity-based partitions were established with *EvoPhylo* (Simões et al. 2023a), using a Gower distance matrix (after randomly resolving polymorphisms) and selecting the optimal number of partitioning around medoids clusters—that is, the one maximizing the silhouette width. Homoplasy-based partitioning was performed following the approach of Rosa et al. (2019). A maximum parsimony tree under implied weighting (IW; Goloboff 1993) was inferred in TNT v.1.5 (Goloboff and Catalano 2016) with a concavity constant of 3 and used to derive character scores. Partitions were built by lumping characters with identical IW scores after rounding to the nearest decimal.

As with molecular data, IQ-TREE was allowed to improve model fit by merging the individual partitions of each original scheme, and the final model comparison was based on the fit of the best nine resulting

schemes (unpartitioned + four original schemes + four merged schemes). Across these, the tree topology was fixed to that obtained using the unpartitioned scheme, and 10 replicates of the entire process were performed. Optimal partitioning and modeling of the morphological matrix was attained with the merged homoplasy-based scheme, which attained a median BIC weight across replicates of 1.0. Further details of morphological model comparison are shown in Supplementary Figure S4. Across-partition rate variation was activated and assigned a flat Dirichlet prior.

Clock and tree models.— The FBD process was employed as a tree prior (Heath et al. 2014; Zhang et al. 2016), using an exponential prior with a rate of 10 for the speciation rate, flat beta priors for relative extinction and fossilization rates, and fixing the fraction of sampled extant taxa to the known value. Ten nodes were constrained (see above) and calibrated using broad offset exponential distributions that were parameterized so as to leave 5% prior probability of origination at times even older than already conservative soft maxima. The same approach was used for the tree age prior. A molecular backbone was enforced for some extant taxa using 17 partial constraints, forcing the recovery of relationships found in genome-scale analyses (Mongiardino Koch and Thompson 2021; Mongiardino Koch et al. 2022); fossil affinities and remaining relationships among extant clades were inferred from the data. All enforced node constraints (calibrated or not) are detailed in Supplementary Table S3. These constraints were placed to allow for a more efficient use of computational effort, as convergence of TED inference can be difficult to attain (see, e.g., May et al. 2021). Previous efforts have shown that most of these nodes are equally supported by morphological and molecular data (Mongiardino Koch and Thompson 2021), and we thus considered that constraining them would allow us to focus on more relevant aspects of uncertainty. Uniform priors accounting for stratigraphic uncertainties and fossil lineage durations were used to calibrate all 95 fossil tips (Barido-Sottani et al. 2020). A diversified taxon sampling strategy was implemented for extant terminals (Höhna et al. 2011), and two sampling strategies were explored for fossils: activating and deactivating their potential recovery as sampled ancestors (Gavryushkina et al. 2014), henceforth referred to as SA and noSA, respectively. The latter was attained by setting to zero the probability of move proposals that would place fossils as direct ancestors, as described in Simões et al. (2020a). It should be noted that both of these strategies assume that fossils are sampled randomly across the tree, whereas both fossil and extant terminals were selected to maximize phylogenetic diversity.

Two types of relaxed clocks were explored: an autocorrelated lognormal model (TK02; Thorne and Kishino 2002), which assumes evolutionary rates are inherited across lineages following a Brownian motion; and an uncorrelated independent gamma model (IGR; Lepage et al. 2007), according to which the evolutionary rates of ancestors and descendants are uncoupled. Across both, a broad normal prior was set for the base rate (normal distribution with mean of 0.001 and standard deviation of 0.01), an exponential prior with rate of 10 was used for the clock variance, and a separate clock was implemented for each data type (morphological, amino acid, and nucleotide) by unlinking relative rates across the corresponding sets of partitions. Although heterogeneous clocks might also exist within each character type (Duchêne et al. 2014; Lee 2016), we assumed this setting captured the most salient aspects of rate variation in our data.

Phylogenetic runs.— Four separate inference procedures were explored varying the type of relaxed clock (TK02, IGR) and the strategy for fossil sampling (SA, noSA) in MrBayes v.3.2.7a (Ronquist et al. 2012b). For each of these, six independent runs composed of four chains each were continued for either 100 million generations with a 25% burn-in fraction (IGR) or 150 million generations with a 50% burn-in fraction (TK02). Sampling was performed every 5000th generation, resulting in 10k posterior samples drawn from each run (60k total for each of the four analytical conditions). Convergence and stationarity of the post burn-in phase were visually confirmed with Tracer v.1.7.1 (Rambaut et al. 2018) and *rwty* (Warren et al. 2017). The average standard deviation of split frequencies ranged between 0.008 and 0.011. Effective sample sizes (ESSs) for all parameters were larger than 170 for TK02 runs and larger than 321 for IGR runs; ESS values for topologies were all above 500. Comparison of posterior median node ages across runs further confirmed adequate levels of convergence (range of Pearson's $\rho = 0.97$–0.99 for IGR runs and 0.94–0.97 for TK02 runs; Supplementary Fig. S5). Analyses were summarized using majority-rule consensus (MRC) and maximum clade credibility (MCC) topologies with median heights; the latter was obtained with TreeAnnotator v.10.5.0 (Drummond and Rambaut 2007) using a random subsample of 15,000 posterior trees per analysis (2500 per run). For some computationally intensive downstream analyses (e.g., treespaces and chronospaces, see below), the set of posterior trees was further downsampled to 1500 per analysis (250 per run).

Analyses of Tree Topology and Divergence Times

Treespaces.— The topological variation induced by the two analytical settings that were changed (i.e., the type of relaxed clock and the strategy for fossil sampling) was explored using treespaces (Hillis et al. 2005; Smith 2022). The number of matching quartets for all pairs of posterior trees was counted and used to derive a symmetric quartet distance using package *Quartet* (Sand et al. 2014; Smith 2019). Distances were then projected onto a

two-dimensional space using multidimensional scaling (MDS).

Chronospaces.— Although treespaces can efficiently summarize topological variation, they cannot portray temporal variation. Efficiently summarizing node age variation is complicated within the context of an analysis that simultaneously estimates topology and divergence times, as posterior chronograms do not share the same set of nodes. We explored two possible solutions to this issue: (A) using the entire tree sample and focusing only on the subset of nodes shared by all and (B) defining a subset of nodes whose frequency [i.e., posterior probability (pp)] exceeds a given threshold, and downsampling the trees to those simultaneously consistent with them all. Clade frequencies were tallied, and those not present in all trees (solution A) or exhibiting frequencies below either 0.95 or 0.90 (solutions B_1 and B_2, respectively) were collapsed. Trees were then downsampled to those retaining the maximum number of nodes (i.e., those consistent with all nodes above the chosen threshold), resulting in data sets of node ages composed of 6k trees/41 nodes (solution A), 3.52k trees/78 nodes (solution B_1), and 1.74k trees/90 nodes (solution B_2). To maintain consistency with the methodology implemented to build treespaces, pairwise Euclidean distances were estimated for each data set and decomposed into two dimensions using MDS. The space obtained for solution A was rotated and scaled using Procrustes superimposition to minimize the sum of squared distances between the coordinates in the chronospace and those in the treespace. These approaches relied on functions from packages *chronospace* (Mongiardino Koch and Milla Carmona 2024) and *vegan* (Oksanen et al. 2024).

Other tree properties.— Across all subsampled posterior trees, we counted the number of taxa placed as direct ancestors (i.e., those with terminal branches of length zero), as well as the overall pp with which each fossil resolved as an ancestor. We also estimated their stratigraphic congruence using the modified Manhattan stratigraphic measure (Pol and Norell 2001), as well as their tree balance (using Colless' index), level of treeness (proportion of total tree length made up of internal branches), and average node support. All five properties were compared across analytical conditions using either analyses of variance or, in the case of the number of sampled ancestors, a generalized linear model with a Poisson error distribution. Code relied on functions from packages *strap* (Bell and Lloyd 2015) and *apTreeshape* (Bortolussi et al. 2006).

Macroevolutionary Inferences

To assess the impact that alternative parameterizations have on downstream analyses, we assessed clade origination times, evolutionary rates, and patterns of morphological change for trees obtained under alternative clock models. For the first, we characterized the general tempo of echinoid diversification through the lens of lineage-through-time (LTT) plots (Harvey et al. 1994), as well as explored the inferred divergence times of some focal clades. For the second, we extracted branch-specific rates of evolution for each of the three data types and tested whether significant differences exist between regular and irregular echinoids—a pattern previously supported using morphological data (Hopkins and Smith 2015)—using Kruskal–Wallis rank sum tests.

Finally, we performed a series of ancestral state reconstructions (ASRs) on the MCC trees of the IGR-SA and TK02-SA analyses. We iterated through every morphological character and pruned the MCC trees to the subset of terminals represented by non-missing, non-polymorphic codings. If the resulting trees contained more than 30 taxa and included members of both Euechinoidea and Cidaroidea (the two sister clades that comprise crown group Echinoidea), model-averaged marginal ASRs were performed for each MCC tree, combining both equal rates and different rates models, and implementing the prior distributions of FitzJohn et al. (2009) for the root node. We then compared the states assigned to the nodes corresponding to the three highest-level crown group clades (Echinoidea and its two descendants: Cidaroidea and Euechinoidea) across both MCC trees, exploring the impact that the implemented clock model has on the reconstruction of morphological evolution across deep time.

Results

Exploration of the posterior trees obtained for the different analyses revealed that major changes in both topology and node ages occur when implementing alternative relaxed clocks. Inference under either autocorrelated (TK02) or uncorrelated (IGR) clocks explored largely disjunct areas of both treespace and chronospace (Fig. 2), indicating a strong and systematic effect of this decision on phylogenetic results. Posterior trees obtained when enforcing a TK02 clock proved less variable, suggesting a narrower region of maximum pp. In stark contrast, preventing fossils from resolving as direct ancestors had no impact on the inference of phylogenetic relationships or divergence times, with topologies including (SA) or excluding (noSA) sampled ancestors entirely overlapping with each other in both treespace and chronospace. This is not modified by exploring a larger fraction of nodes ages (Supplementary Fig. S6). Decomposing total variance using a between-group principal component approach (as implemented in *chronospace*) reveals the same picture: varying the clock model accounts for 27.8% of variance in treespace and 60.8% of variance in chronospace, whereas varying the fossil sampling strategy explains less than 0.2% in either.

Direct ancestry was relatively common among the posterior trees inferred using an uncorrelated relaxed

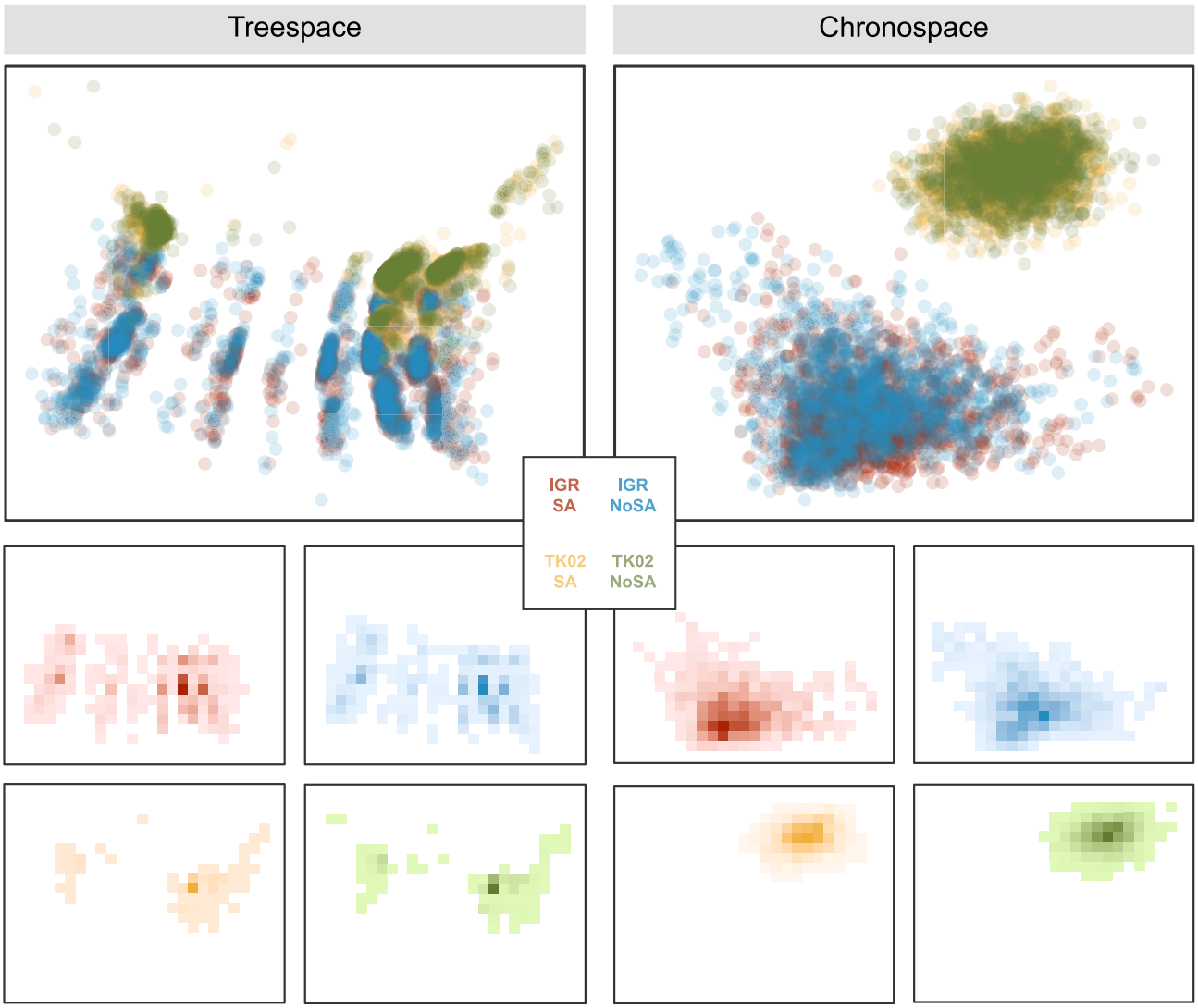

FIGURE 2. Treespace and chronospace condensing topological and temporal variability (respectively) across a random subsample of posterior trees obtained under the four analytical conditions explored. Analyses are colored as shown in the legend (center). The bottom panels show the same data using separate heatmaps for each analytical condition. Although analyses implementing different clocks (TK02, IGR) resolve in different areas, those varying the fossil sampling strategy (SA, noSA) are completely superimposed, evidencing no effect of the latter on phylogenetic results.

clock (i.e., in the IGR-SA analysis). A median number of nine terminals per posterior tree resolved as sampled ancestors of other clades, with a 95% confidence interval (CI) between 5 and 13 (Fig. 3a). Nonetheless, as shown in Figure 2, IGR-SA and IGR-noSA analyses do not differ topologically or temporally; across these analyses, a fraction of fossil tips resolved as either direct ancestors or sister taxa of the same clades, without these alternative ways of attaching to the same branch modifying topology or divergence times in any substantial way. Lineages with fossils placed as direct ancestors under the IGR-SA analysis are summarized in Figure 4a. On the contrary, when an autocorrelated relaxed clock was enforced, no terminals were recovered as sampled ancestors, even when allowing for them (i.e., in the TK02-SA analysis). In fact, the median posterior value for the parameter describing the proportion of fossils recovered as ancestors in this analysis was zero, compared with a median value of 0.095 (95% CI: 0.053–0.137) for the IGR-SA analysis. Given these results, subsequent comparisons focus only on the IGR-SA and TK02-SA trees. Further systematic differences are evident between these two analyses (Fig. 3a), with posterior trees obtained under an autocorrelated relaxed clock exhibiting significantly lower stratigraphic congruence, level of treeness, and tree balance, while also showing significantly higher

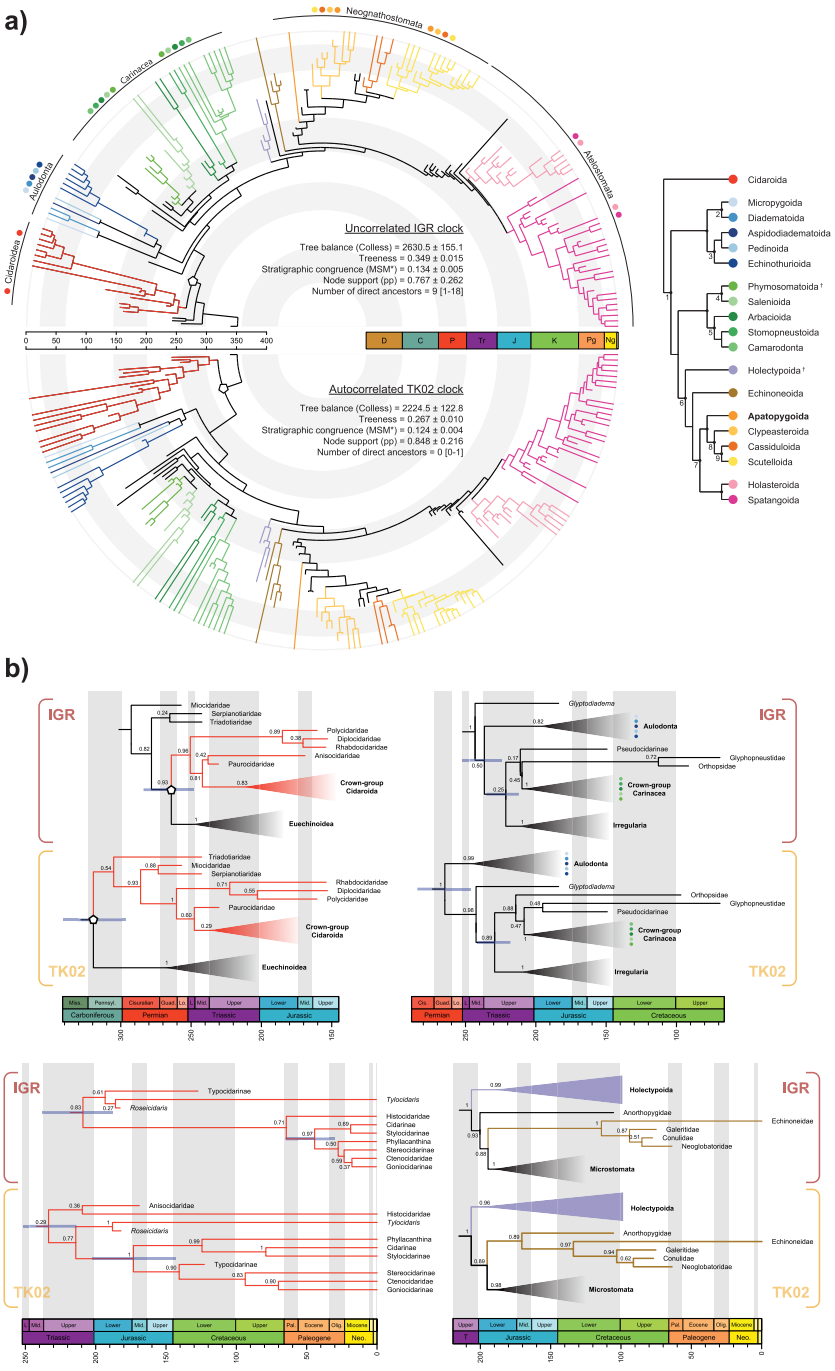

FIGURE 3. Comparison of TED chronograms obtained under uncorrelated (IGR-SA) and autocorrelated (TK02-SA) clock models. a) Summary of differences between the MCC trees obtained under both analytical conditions. Clades recognized at the level of order are colored and named on the cladogram (top right); other higher-level clades are shown using either peripheral brackets on the chronogram or numbered nodes on the cladogram. Apatopygoida is shown in bold to highlight its previously unrecognized status at the level of order. Properties estimated across both sets of posterior trees are shown in the center, as either mean ± standard deviation or median [range]. Here and throughout, a pentagon is used to identify the node of crown group Echinoidea. Numbered nodes on the cladogram: 1. Euechinoidea, 2. Diadematacea, 3. Echinothuriacea, 4. Calycina (sensu Kroh 2020), 5. Echinacea (sensu Kroh 2020), 6. Irregularia, 7. Microstomata, 8. Luminacea, and 9. Echinolampadacea. Names for unnumbered nodes marked with a black circle are labelled on the chronograms. Crosses denote orders that are entirely extinct. b) Highlights of major differences between both MCC trees: top left, origin of crown group Echinoidea; top right, major euechinoid clades; bottom left, relationships and divergence times within crown group Cidaroida; bottom right, early diversification of irregular echinoids. Values on nodes are posterior probabilities; node age uncertainty for some clades of interest is shown using 95% highest posterior density intervals (see main text for explanation).

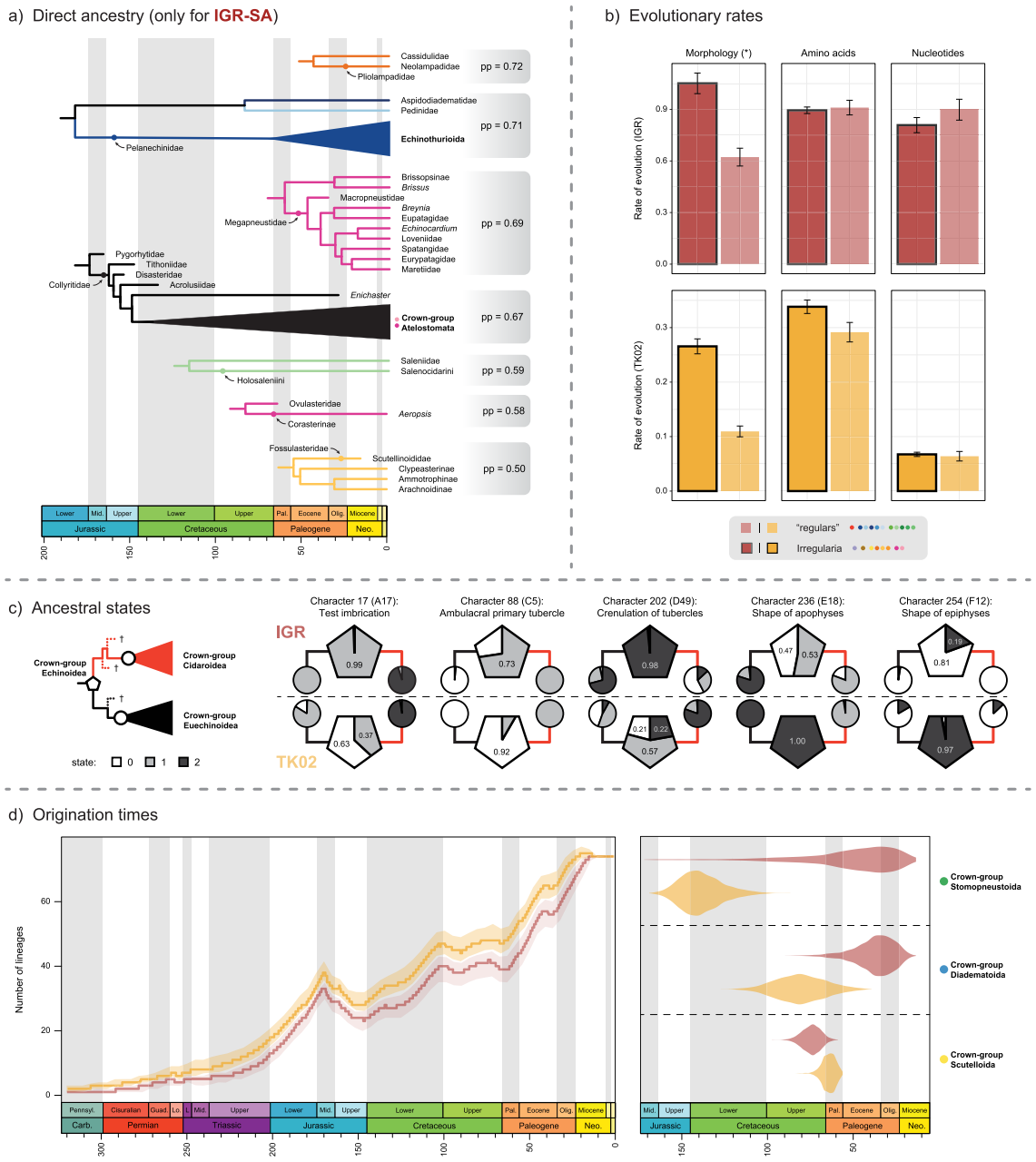

FIGURE 4. Consequences of clock choice for downstream evolutionary inferences. a) Lineages with strong evidence (pp > 0.5) of being direct ancestors. Although TK02-SA analyses allowed for the placement of fossils as direct ancestors, no such relationship was recovered. Branch colors follow those of Figure 3. b) Branch-specific evolutionary rates for the three data types (morphology, amino acids, and nucleotides), across "regular" echinoids and Irregularia. Significant differences ($P < 0.05$) are denoted by an asterisk. Top (red) bars represent values from the IGR-SA condition, and bottom (yellow) ones from the TK02-SA condition. c) ASR of morphological traits for the nodes corresponding to the crown groups Echinoidea (pentagon), Cidaroidea (circle, red branch), and Euechinoidea (circle, black branch), in the MCC trees of the IGR-SA and TK02-SA analyses. These nodes are identified as the last common ancestor shared by all extant descendants and might also include different numbers of fossil lineages (as shown in the diagram on the left using dotted branches leading to terminals marked with a cross). Values within pentagons represent ML probabilities of each state. Characters are identified by their position in the morphological matrix used here, their code in Kroh and Smith (2010), and a brief description. Full details can be found in Supplementary Figure S9. d) Impact of the clock on reconstructed patterns of echinoid diversification, including LTT curves (left) and posterior age densities for selected nodes (right). The LTT plot shows median node age values and LOESS-smoothed 95% CIs. Data in red correspond to the IGR-SA condition, and data in yellow to the TK02-SA condition. LTT plots for posterior trees pruned to include only extant terminals are shown in Supplementary Figure S10. The posterior node age densities highlight three crown group orders which are inferred to originate either before or after the Cretaceous-Paleogene (K-Pg) mass extinction event depending on the clock implemented. Median inferred node ages for all comparable clades can be found in Supplementary Figure S11.

node support values (consistent with the reduced variability seen in the treespace of Fig. 2).

Analyses further differed in crucial phylogenetic details, summarized in Figure 3b. Under an IGR clock, crown echinoids are dated to the Guadalupian (middle Permian), with a 95% highest posterior density (HPD) interval that encompasses post Permo-Triassic (P-T) mass extinction times. In contrast, a TK02 clock places this node decidedly within the Carboniferous, representing a difference in median inferred origination times of 55.6 Ma, and excluding the possibility of a post P-T origination. Earlier times of origin are accompanied by the incorporation within the crown group of the late Permian/early Triassic members of the families Miocidaridae, Serpianotiaridae, and Triadotiaridae, lineages that otherwise resolve as stem group taxa (Fig. 3b, top left). TK02 analyses also result in older ages for the two main lineages of crown group echinoids—Euechinoidea and Cidaroidea—and within the latter, of Cidaridae, which is dated to either 172.2 Ma (95% HPD: 141.3–202.3 Ma; TK02) or 45.7 Ma (95% HPD: 30.7–65.8 Ma; IGR). These alternatives are also accompanied by changes in relationships, not just for fossil taxa (examples of which include the placement of *Glyptodiadema*, Anisocidaridae, and Typocidaridae) but also for extant lineages, including whether histocidarids or psychocidarids (the latter represented by both *Roseicidaris* and *Tylocidaris*) constitute the sister group to the remainder of crown group Cidaroida. Within Irregularia, different clocks support the existence of either two clades of stem group irregulars—Holectypoida and Anorthopygidae—or just one, with anorthopygids resolving instead as an early member of the extant Echinoneoida (Fig. 3b, bottom right). Despite these striking differences, order-level relationships are consistent among analyses, and are summarized on the cladogram of Figure 3a. MCC and MRC trees for both IGR-SA and TK02-SA inference conditions, including 95% HPD intervals and posterior probabilities, can be found in Supplementary Figures S7 and S8, respectively. Some terminals previously excluded due to their instability are resolved consistently across analyses (e.g., *Enichaster*, which is strongly supported as the sister clade to crown group Atelostomata, Supplementary Figures S7 and S8) evidencing the stability provided by stratigraphic and/or molecular data to morphological rogue taxa.

A few nodes whose inferred ages proved remarkably sensitive to the implemented clock are shown in Figure 4d, involving three crown group clades that are dated to times at either side of the Cretaceous-Paleogene (K-Pg) mass extinction by different clocks. Although TK02 showed a general tendency to favor older divergence times, a handful of nodes are pushed forward under this clock, including that corresponding to crown group sand dollars (Scutelloida). Divergence times for all comparable clades across both clocks are shown in Supplementary Figure S11. While the effect of the implemented clock model on branch durations is pervasive, it does not greatly modify general patterns of diversification (Fig. 4d) or estimates of evolutionary rate variation among major lineages (Fig. 4b). Irregular echinoids are confirmed to be characterized by significantly higher rates of morphological evolution (as also shown in Hopkins and Smith 2015), yet these are accomplished in the absence of elevated molecular rates. One downstream inference that did show high analytical sensitivity was that of the ancestral states reconstructed at the origin of crown group Echinoidea. Thirteen morphological traits differed in the most probable state assigned to said node, five of which are highlighted in Figure 4c (and fully explained in Supplementary Fig. S9). Not only do these trees imply different locations for the origin of key morphological innovations, but they occasionally also differ on which of the two major extant lineages bears the ancestral condition (e.g., characters 88 and 236).

Discussion

Improving TED of Echinoidea

Bayesian methods of TED that implement relaxed clocks and FBD processes are regarded as the gold standard for the simultaneous inference of tree topologies and divergence times. These approaches combine numerous benefits, including a reliance on mechanistic models describing all aspects of the underlying evolutionary dynamics, as well as an ability to combine all available sources of information (and their intrinsic uncertainties). They can also produce chronograms that sample thoroughly across both living and extinct diversity in a manner conducive to accurate macroevolutionary inferences. The behavior of TED approaches under simulation conditions is well characterized, and they have been extensively implemented in empirical studies of vertebrates (e.g., Beck and Lee 2014; Arcila et al. 2015; Lee 2016; Pyron 2017; Gavryushkina et al. 2017; Lee and Yates 2018; Simões et al. 2020b; Tejada et al. 2024) as well as a handful of clades of arthropods (e.g., Ronquist et al. 2012a; Sharma and Giribet 2014; Zhang et al. 2016; Gustafson et al. 2017; Gainett et al. 2024) and plants (e.g., May et al. 2021; Coiro et al. 2023; Flores et al. 2023). Even though echinoderms offer unique advantages to utilize—and test—these methodologies, they remain relatively unexplored. Our goal here was to expand upon the only echinoderm TED analysis previously performed, the study of Mongiardino Koch and Thompson (2021) on Echinoidea, using improved methodologies, better sampled data sets, and an exploration of the effects of some analytical decisions.

The aforementioned study had incorporated transcriptomic data for 27.6% of extant terminals, a value that was increased here to 42.9%, and further raised to a value of 82.8% of extant terminals with some amount of molecular information through the addition of Sanger-sequenced data. This reveals the sustained relevance of these legacy data sets in the genomic era, especially for

taxa that will remain difficult to sample and preserve in optimal conditions, as is the case for many deep-sea invertebrates. Mongiardino Koch and Thompson (2021) had also relied on a partitioning scheme for morphological data that was based on the number of character states (Gavryushkina et al. 2017; Mulvey et al. 2025), an approach that ensures that characters are assigned a transition matrix of appropriate dimensions (although see Khakurel et al. 2024), but can also suffer from issues of character weighting (King et al. 2017). Recent years have seen an appraisal of the importance of accurately modeling morphological data, as well as the development of new algorithmic approaches to character partitioning (Lanfear et al. 2017; Rosa et al. 2019; Azevedo et al. 2022; Casali et al. 2022; Simões et al. 2023a) that tend to fit the data better than either unpartitioned or anatomy-based partitioning. Our results broadly align with previous efforts, confirming that partitioning morphological data always improves model fit (Clarke and Middleton 2008; Tarasov and Genier 2015), and that homoplasy-based methods outperform other alternatives (see Supplementary Fig. S4; Rosa et al. 2019; Casali et al. 2022; Lepeco and Melo 2024). The latter result makes sense, as the restriction of model space for morphological data to variants of the Mk renders partitioning an exercise in finding the best way of modeling among-character rate variation (i.e., allowing for it to be subdivided into rate variation between and within partitions, modeled by rate multipliers and gamma distributions, respectively). Further research should explore how different IW concavities affect the recovery of meaningful partitions. Depending on the software employed, these partitioning schemes must be further modified to ensure that transition matrices are correctly specified (MrBayes enforces this automatically). Finally, it should be pointed out that all original schemes were improved by a subsequent step of partition merging, which we argue should become standard as the modeling of morphological data continues to evolve to resemble that of molecular data sets, both in complexity and automatization.

The other main difference with respect to previous efforts was the implementation of an FBD tree prior, supplanting the use of the improper uniform tree prior (May et al. 2021). This prompted a number of decisions, among them the implemented strategy for fossil taxon sampling. FBD processes can infer ancestor-descendant relationships among sampled taxa directly from the data, improving the modeling of diversification history for epidemiological and paleontological data sets for which sampled terminals do not necessarily arise through cladogenesis (Gavryushkina et al. 2014). Empirical efforts have shown that direct ancestors are likely common among known fossil species (Foote 1996; Parins-Fukuchi and Saulsbury 2025), and that recognizing that speciation might occur through mechanisms other than strict bifurcation can affect our understanding of diversification dynamics (Crouch et al. 2021) and trait evolution (Caetano and Quental 2023). Nonetheless, direct ancestry should probably only be accommodated if one expects such relationship to be present in the data (Simões et al. 2020a), a probability that should decrease when sampling is sparse, focused on higher-level terminals, and spanning a vast period of time—conditions that are all met here (but see below). A similar logic applies to the choice of relaxed clock: autocorrelation (i.e., the inheritance of evolutionary rates) is a sensible biological expectation (Gillespie 1984; Tao et al. 2019), yet this pattern can be entirely eroded by a sparse taxon sampling. To our knowledge, only the morphological tip-dated study of sphenodontian reptiles by Simões et al. (2020a) had assessed sensitivity to both of these factors, and their concomitant effect on TED inference had never been explored before the present study.

Impact of Relaxed Clocks and Direct Ancestry

Our results reveal a striking asymmetry in the impact exerted by the two methodological decisions varied, with the type of clock greatly affecting both topology and divergence times, whereas accommodating direct ancestry shows no effect (Fig. 2). Although the former has been long appreciated (e.g., Ronquist et al. 2012a; Zhang et al. 2016; Tejada et al. 2024), the latter is surprising. Previous analyses based on morphological data sets had found that allowing for direct ancestry substantially modified divergence times (Bapst et al. 2016; Simões et al. 2020a), resulting in older node ages as the total morphological disparity of a clade must arise from evolutionary processes operating within fewer phylogenetic branches. Although allowing for direct ancestry also had an effect on the age of one focal node in a TED analysis (Gavryushkina et al. 2017), the magnitude of change was comparatively small and in the opposite direction (i.e., favoring slightly younger nodes). It seems likely that as morphological data represent a progressively smaller fraction of total-evidence data sets, the alternative placement of a given fossil as either a direct ancestor or a sister clade will have less of an effect on the amount of change reconstructed for the attachment branch. Although further research should clarify if this result is data set-specific, we believe that—within the context of large-scale TED inferences—direct ancestry might be amenable to accommodation without affecting branch durations, and therefore have no consequence for divergence time estimation.

On the other hand, the recovery of fossil terminals as direct ancestors was entirely contingent on the relaxed clock implemented, revealing an extreme case of interdependence between the modeling components of Bayesian dating. Under the autocorrelated TK02 relaxed clock, only 0.1% of posterior trees contained sampled ancestors, and the few that did exhibited only a single ancestor-descendant pair; in comparison, all posterior trees contained sampled ancestors under the uncorrelated IGR clock, with numerous taxa placed with confi-

dence as direct ancestors of other lineages (Fig. 4a). It is worth noting that previous morphological phylogenies of major echinoid clades explicitly depicted both direct ancestry and budding cladogenesis (Smith 2007; Kroh and Smith 2010), the second of which could be reduced to direct ancestry if long-lived lineages were constrained temporally to the stratigraphic range of a single coded species, as done here. One such relationship implied by Kroh and Smith (2010) and corroborated here is that between Corasterinae and Aeropsidae, represented here by its sole extant genus *Aeropsis* (Fig. 4a). Similarly, previous authors had suggested that Echinothuriidae arose "through" the Jurassic genus *Pelanechinus* (Durham and Melville 1957; Smith 2015), and highlighted the extent to which its morphology appeared to be "transitional" between lineages now recognized as the main branches of extant Aulodonta (Groom 1887; Philip 1965). These ideas are validated by our results, which place Pelanechinidae as a direct ancestor along the stem of Echinothurioida. Finally, the morphology of other terminals (e.g., Fossulasteridae and Scutellinoididae) is similar enough that their recovery as ancestor-descendant pairs—given the fact that they were assigned disjunct stratigraphic ranges—constitutes a sensible outcome. Although a strict interpretation of direct ancestry might not always be warranted when working with terminals above the species level, the ability to infer trees in which lineages can explicitly evolve through sampled ancestral morphotaxa might still be beneficial, and is certainly consistent with how paleontologists have interpreted a number of these clades.

The ability to infer direct ancestry, nonetheless, was only realized in this study when uncorrelated rates of evolution were assumed. We caution that this result might stem from factors that are both data set- and software-specific (or a combination thereof), with more research needed to pinpoint its causes. A previous TED study on the higher-level relationships of hymenopteran insects (also performed in MrBayes) had indeed succeeded in recovering direct ancestors under a TK02 clock, although they also found this type of relationship to be much more common when implementing an IGR clock (Zhang et al. 2016). The elevated frequency of direct ancestors under IGR was considered implausible and attributed to a high prior probability of direct ancestry that an uninformative morphological partition was unable to override. This explanation does not seem to apply here. First, the number of taxa involved in direct ancestry under IGR is not only reasonable, but in fact much smaller than the number of non-cladogenetic originations assumed for this same set of terminals by Kroh and Smith (2010). Furthermore, our morphological data set is highly informative, supporting topologies that are relatively consistent with phylogenomic ones (barring a handful of exceptions; Mongiardino Koch et al. 2018, 2022; Mongiardino Koch and Thompson 2021), and that exhibit levels of missing data among extinct taxa that are low and comparable to those of extant ones. Instead, we suggest an alternative explanation for this phenomenon: current implementations of autocorrelated clocks might unduly disfavor the inference of direct ancestry, as forcing evolutionary rates to change following a Brownian motion complicates the recovery of branches of zero length. Under this scenario, a jump from a measurable (i.e., non-zero) ancestral effective branch length to a null one in a descendant (needed for the latter to be placed as a sampled ancestor) might be beyond what the model can allow. In this study, this would have to happen independently for all three implemented clocks (given that fossil terminal branches also have effective branch lengths for molecular partitions), something that the model does not seem to accommodate. Once again, this phenomenon could be data set-specific, driven by factors such as the low level of occupancy across nucleotide and amino acid alignments (across which 62% of terminals, all fossils plus 14 extant OTUs, are entirely missing), the sparse sample of taxa from such an ancient and diverse lineage, and the use of amino acid data, which remains rarely employed in TED and seems to exhibit lower among-lineage rate variation than either morphology or nucleotides (Supplementary Fig. S12), making large jumps in rates even less likely. On the other hand, another potential factor for why this result was not previously recovered could be the lack of availability of some of these models across software. For example, most sampled-ancestor FBD analyses to date have been performed using the BEAST/BEAST2 family of software, which have not consistently implemented autocorrelated clocks, thus preventing a thorough exploration of model sensitivity.

As already mentioned, the impact of the relaxed clock extends well beyond the recovery of direct ancestry, resulting in a different balance between stratigraphy and character data (King 2021), and having broad phylogenetic and macroevolutionary consequences (Figs. 2–4). We believe most of these to be driven by alternative clocks differing in the way they accommodate variation in molecular rates among lineages, not just because molecular data constitute most (97.4%) of the data set, but because similar differences were previously found when using alternative clocks within the context of node dating (Mongiardino Koch et al. 2022). For example, median node ages for Cidaridae obtained here range between 44 and 173 Ma, values that are highly consistent with the age range of 51–147 Ma previously obtained for this clade when node dating under different clocks (Mongiardino Koch et al. 2022). The only factor in common between these studies is that inference was performed under both autocorrelated and uncorrelated clocks—Mongiardino Koch et al. (2022) did not incorporate fossils, had no morphological data, used a much larger molecular data set, and employed both a different software and tree prior. Cidarids (and potentially all cidaroids) have significantly lower rates of molecular evolution than all other extant echinoids (Mongiardino Koch et al. 2018). In the absence of node age constraints

for the clade, their time of origin is mostly determined by the ability of the relaxed clock to successfully model shifts in evolutionary rates, a scenario under which uncorrelated clocks can favor dates that are systematically underestimated (Crisp et al. 2014). In this study, we also obtain a general pattern of younger ages under the IGR clock (Supplementary Fig. S11), yet in the absence of model fitting efforts, it is dangerous to interpret these as biased. Although one would hope that the temporal information present in the tip ages of fossil cidaroids would help further constrain their origins, the general uninformativeness of cidaroid morphology (Kroh and Smith 2010; Hopkins and Smith 2015; Smith 2015; Mongiardino Koch and Thompson 2021) causes these taxa to vary widely in their phylogenetic placement (Fig. 3b), moving in and out of clades as these are dated to older (TK02) or younger (IGR) times, respectively. The same seems to happen with three fossil clades—Miocidaridae, Serpianotiaridae, and Triadotiaridae—variously considered by previous authors as either stem group echinoids, cidaroids, or euechinoids (and thus, potentially among the earliest crown group lineages; Durham and Melville 1957; Philip 1965; Smith 1990, 1994, 2007; Kroh and Smith 2010; Mongiardino Koch and Thompson 2021). Their morphology is relatively consistent with any of these interpretations, so their position is mostly determined by the inferred ages of surrounding nodes. These various topological and temporal changes lead to alternative scenarios of the evolution of key aspects of echinoid morphology (Figs. 4c and S9). These include the nature of the perignathic girdle (the structure supporting the muscles used for feeding) in the most recent common ancestor of extant echinoids, as well as whether or not their test was tightly sutured (as that of most living forms), or relatively flexible and made of imbricating plates (as in many Paleozoic stem-group lineages). These different optimizations either validate or negate long-discussed putative synapomorphies of crown group Echinoidea, as well as inform on the extent to which living cidaroids, which have long been considered to display plesiomorphic character states, resemble the last common ancestor of crown group echinoids (Smith 1981, 1984; Smith and Hollingworth 1990; Thompson et al. 2015, 2020).

The Phylogeny of Echinoidea and the Path Ahead

Despite all of these uncertainties, our results support a robust scheme of relationships among the major branches of the echinoid tree of life (Fig. 3a), as well as a consistent history of diversification through time (Fig. 4d). The recovery of the extant Apatopygidae as an early offshoot of the diversification of irregular echinoids is congruent with previous phylogenomic efforts (Mongiardino Koch et al. 2022), and confirms that the clade is unrelated to other extant "cassiduloids," a result that was likely previously obtained due to the general difficulty of accurately placing long-lived, slow-evolving taxa when performing morphological tip dating (Turner et al. 2017; King 2021; Mongiardino Koch and Thompson 2021; Mongiardino Koch et al. 2023). Although morphological similarities between apatopygids and nucleolitids had been highlighted as potential evidence of a close relationship (Mortensen 1948; Kier 1966; Suter 1994; Souto et al. 2019; Mongiardino Koch et al. 2022), these clades emerge as independent offshoots of the early neognathostomate diversification (as was also suggested by Kroh and Smith 2010). Accordingly, we recognize Apatopygoida as a new order (see below).

Although much work is still needed at lower taxonomic levels, few uncertainties remain regarding the emergence of the major clades of echinoids. Only one set of relationships, the earliest split among extant Carinacea, has proved sensitive to the data set and implemented methodology. Although Salenioida occupies that position here, in agreement with morphological signal (Kroh and Smith 2010), phylogenomic efforts revealed a stronger but ambiguous signal for Arbacioida to occupy that position (Mongiardino Koch et al. 2022). Furthermore, Echinoneoida remains the only extant order whose placement has not been addressed using genome-scale data sets, and for which more than one possible location has been previously obtained (as either the sister group to all other extant irregulars, or just to neognathostomates; Kroh and Smith 2010; Mongiardino Koch and Thompson 2021). Although improvements in topological resolution among less divergent extant clades will advance as more molecular data become available (e.g., Lee et al. 2023; Minin et al. 2024), their interrelationships with extinct lineages will likely continue to hinge on modeling choices, especially for regions of the tree for which morphology has proven less informative.

Recognition of a New Extant Order of Echinoidea

Apatopygoida new order.—

Diagnosis. As for the family (see Kier 1962), with the provision that all individual features listed are shared with various early fossil neognathostomates that are not included within the clade. The order can be diagnosed by the unique combination of the following traits: periproct in deep sulcus entirely contained on aboral surface, ontogenetic change from tetrabasal apical system in juveniles to monobasal in adults, unipores for tube feet between ends of petals and peristome (including phyllode), poor development of bourrelets, presence of "pyrinid" plating between the petals and the peristome, and absence of any trace of "naked zone" (sensu Mooi 1990).

Included taxa. Only the family Apatopygidae (Kier 1962), as currently diagnosed. The type genus is *Apatopygus* (Hawkins 1920), for which *A. recens* (Milne Edwards 1836) is the type species (Fig. 5). There are

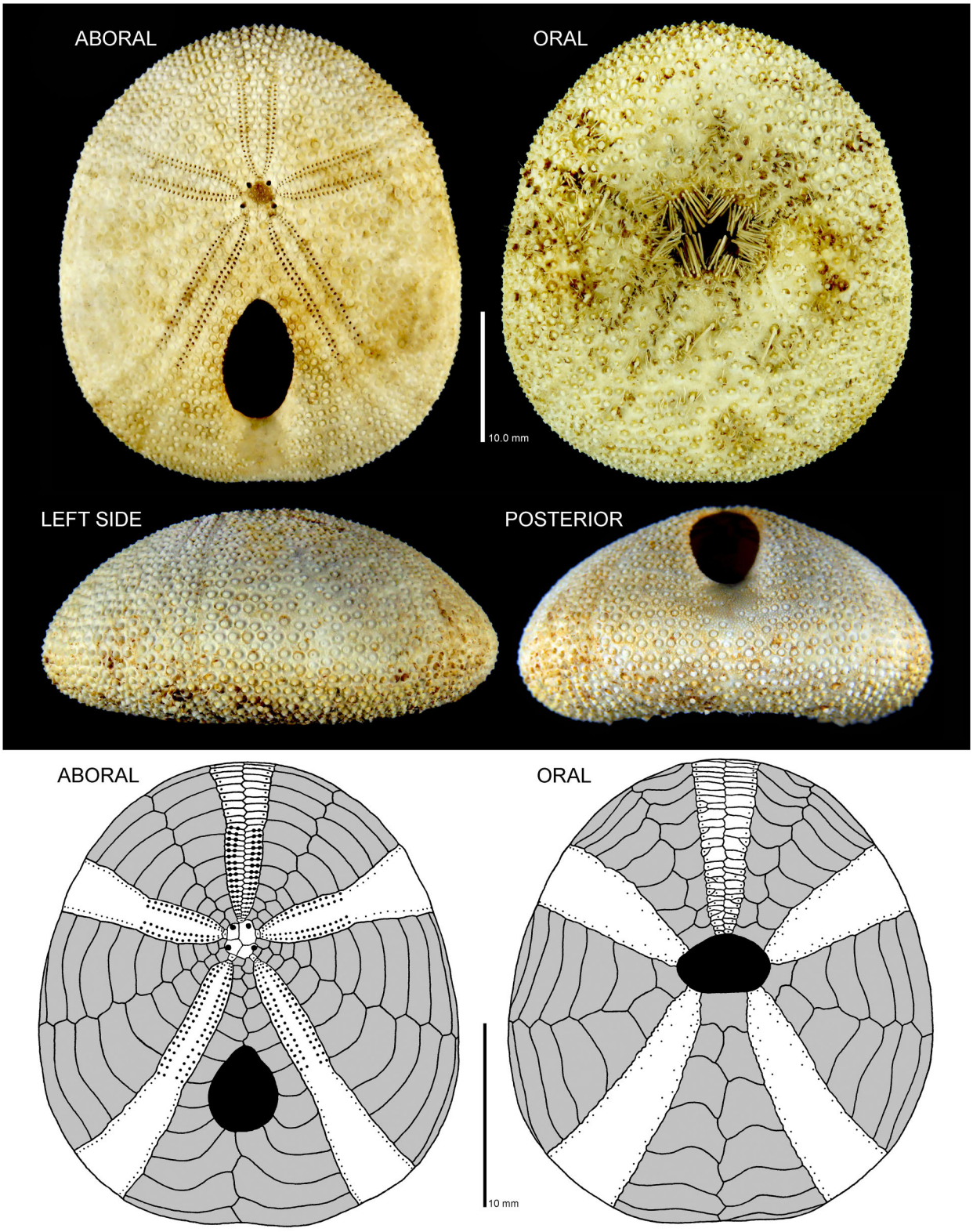

FIGURE 5. Morphology of *Apatopygus recens* (Milne Edwards 1836). Photographs are of specimen EcEs 5107, Museum National d'Histoire Naturelle of Paris. Architectural plate maps of the test correspond to specimen E16325, US National Museum of Natural History. Peristome and periproct are in solid black, and interambulacra are shaded. Details of ambulacral plating are shown only for the anterior ambulacrum.

three extant species: *Apatopygus recens* (Milne Edwards 1836), *Apatopygus occidentalis* (H.L. Clark 1938), and *Porterpygus kieri* (Baker 1983). Extant species of *Apatopygus* are presently known only from New Zealand and southwestern Australia, and *Porterpygus* only from New Zealand. Fossil taxa in these genera have been described from the Late Oligocene to Middle Miocene of Australia (Holmes 1999). Apatopygidae also includes the European Cretaceous genera *Jolyclypus* (two nominal species) and *Nucleopygus* (approximately 16 nominal species), as listed in Kroh and Mooi (2024). However, Saucède and Néraudeau (2006) placed *Jolyclypus* as a subgenus within *Nucleopygus*.

Remarks. Here, we establish a new order to accommodate the family Apatopygidae (Kier 1962) to the level of order. The name Apatopygoida has been published, but without explanation by accompanying text. For example, the word "Apatopygoida" (and its variant "apatopygoids") appears in Kroh and Smith (2010; Figs. 2 and 4). However, no formal description of Apatopygoida was provided, and the clade was recognized instead at the family level in the same publication. The name is absent from subsequent classifications (Kroh 2020; Kroh and Mooi 2024), so the term Apatopygoida in work prior to the present revision is a *nomen nudum*.

Diagnoses for the family given in Kier (1962) and Holmes (1999) are incorrect in stating that buccal pores are absent, because pores homologous to the buccal pores found in all other neognathostomates are clearly discernible (RM, unpublished observations), and can be seen in the illustrations of both *Apatopygus* and *Porterpygus* given in Holmes (1999) as well as herein (Fig. 5). Much importance has been given to a supposedly unique apatopygid character known as "pyrinid" plating in the ambulacra, in which two primary plates are followed more or less regularly by an abradially placed demiplate (Fig. 5). However, this pattern is also seen in non-apatopygids, notably holectypoids. The change from a tetrabasal to monobasal apical system during ontogeny requires additional study, as at least some specimens appear to retain a tetrabasal apical system relatively late in ontogeny (Fig. 5).

The present taxonomic change highlights the uniqueness of the apatopygoids, which last shared a common ancestor with the remainder of extant Neognathostomata (sand dollars, sea biscuits, and allies) deep in the Mesozoic. As presently understood, none of the members of the Apatopygoida is found in strata older than the Cretaceous. The morphological similarities between them and nucleolitids appear to be largely superficial, based on gross morphology of the test, and likely symplesiomorphic, such as the presence of the periproct within a sulcus. More significant is the fact that the tube foot pores are unipores in the phyllodes of apatopygoids and other taxa crownward to them. In nucleolitids and other earliest neognathostomates, the tube feet outside of the petals are supported by bipores. Moreover, in apatopygoids, the apical system is monobasal in some adults, but tetrabasal in nucleolitids. The fact that juvenile apatopygoids preserve tetrabasality suggests derivation from a configuration similar to that of nucleolitids and other early neognathostomates.

Although there is strong molecular support for the placement of extant Apatopygoida, caution is warranted for its fossil members. The apatopygoid fossil record evidently begins much later than that of the nucleolitids, as well as markedly postdating their times of origin as inferred here. Although the overwhelmingly plesiomorphic morphology of both apatopygoids and phylogenetically-adjacent lineages complicates their study, revisionary taxonomic and phylogenetic work could result in a reallocation of known taxa, thereby filling gaps in both their stratigraphic ranges and their evolutionary history.

Conclusions

Here, we focused on combining large-scale morphological, molecular, and stratigraphic data sets for the major lineages of Echinoidea, and analyzing them using state-of-the-art phylogenetic methods. Despite working at the edge of what is currently computationally feasible within the realm of Bayesian TED (involving year-long run times on a high-performance computer cluster), we find that key aspects of our results remain contingent upon methodological decisions that are seldom explored or justified. Within the context of tip dating, model selection approaches for validating the choice of relaxed clock (such as Bayes factors) have generally succeeded for morphological (Lee et al. 2014; Dembo et al. 2016; Simões et al. 2020a) and small-scale total-evidence analyses (Casali et al. 2020); yet the few large-scale TED studies that attempted this were met with uncertainty (Ronquist et al. 2012a). This highlights the need for a careful assessment of sensitivity; in fact, many of the results shown here to hinge upon the choice of clock model (e.g., the composition of the earliest splits within the echinoid crown group) were previously hailed by some of us as novel phylogenetic results made possible by TED (Mongiardino Koch and Thompson 2021). The impact of this methodological choice goes beyond changes in tree topology and divergence times, as it can modify downstream macroevolutionary inferences, affecting our understanding of the congruence between phylogeny and stratigraphy, and even limiting our ability to recover fossils as direct ancestors.

After molecular data grew in availability and genome-scale data sets became the foundation upon which phylogenetic relationships, divergence times, and macroevolutionary patterns were routinely inferred, TED was received as a means of integrating once again the irreplaceable information that the fossil record provides to understanding evolutionary history (Lee and Palci 2015; Pyron 2015). Our results challenge this view, showing instead that fossil terminals can some-

times remain largely relegated. In our analyses, this occurs predominantly within regions of the tree characterized by a relatively uninformative morphological signal coupled with stark variations in molecular rates. Under these conditions, characteristic of the echinoid stem group and early diversification of cidaroids, fossil tips fail to provide enough information to constrain node ages, which become instead determined by the clock model. This happens despite working close to the upper limit of morphological data set sizes for invertebrates (Mulvey et al. 2025), and thus we believe this might be a relatively common phenomenon in total-evidence phylogenetics. Our understanding of the phylogenetic affinities of key fossils across the tree of life, and their ability to inform macroevolutionary history, might thus be contingent upon modeling assumptions regarding rate inheritance among characters they do not even possess.

Acknowledgments

This manuscript benefitted from discussions about molecular clocks and direct ancestry with Tiago R. Simões and April M. Wright, as well as comments from Sebastian Höhna, Seraina Klopfstein, Raquel López-Antoñazas, Joseph Keating, and Ivan Magalhaes. We also want to thank Sonja Huč and Marina McCowin for DNA extractions and PCR amplifications, Natasha Picciani for help with the use of scripts for orthology inference, and Ferdinand Marlétaz and Yuwu Chen (San Diego Supercomputer Center) for computational assistance. The beginning of the title of this article is taken from the 1971 song "The Musical Box" by Genesis.

Supplementary material

Data available from the Dryad Digital Repository: http://dx.doi.org/10.5061/dryad.xgxd254s5

Conflict of interest

None declared.

Funding

This work was funded by National Science Foundation (NSF) through grants DEB-2036186 and DEB-2036298 to G.W.R. and R.M., respectively. J.R.T. was funded by a Leverhulme Early Career Fellowship.

Data availability

Newly generated molecular data are available from GenBank with accession numbers PQ619100–PQ619108. Accession numbers for all preexisting molecular data are listed in Supplementary Table S1. The *deWoRMr* R script is available from GitHub: https://github.com/mongiardino/deWoRMR. All data and code used in this analysis are deposited on the Dryad Digital Repository: https://doi.org/10.5061/dryad.xgxd254s5.

References

Agassiz A. 1879. Preliminary report on the Echini of the Exploring Expedition of HMS "Challenger". Sir C. Wyville Thomson Chief of Civilian Staff. Proc. Am. Acad. Arts Sci. 6(14):190–212.

Arcila D., Pyron R.A., Tyler J.C., Ortí G., Betancur-R R. 2015. An evaluation of fossil tip-dating versus node-age calibrations in tetraodontiform fishes (Teleostei:Percomorphaceae). Mol. Phylogenet. Evol. 82:131–145.

Arndt A., Marquez C., Lambert P., Smith M.J. 1996. Molecular phylogeny of eastern Pacific sea cucumbers (Echinodermata:Holothuroidea) based on mitochondrial DNA sequence. Mol. Phylogenet. Evol. 6(3):425–437.

Azevedo G.H.F., Bougie T., Carboni M., Hedin M., Ramírez M.J. 2022. Combining genomic, phenotypic and Sanger sequencing data to elucidate the phylogeny of the two-clawed spiders (*Dionycha*). Mol. Phylogenet. Evol. 166:107327.

Baker A.N. 1983. A new apatopygid echinoid genus from New Zealand (Echinodermata: Cassiduloida). National Museum of New Zealand Records. 2:163–173.

Bapst D.W., Wright A.M., Matzke N.J., Lloyd G.T. 2016. Topology, divergence dates, and macroevolutionary inferences vary between different tip-dating approaches applied to fossil theropods (*Dinosauria*). Biol. Lett. 12(7):20160237.

Barido-Sottani J., Pohle A., De Baets K., Murdock D., Warnock R.C.M. 2023. Putting the F into FBD analysis: tree constraints or morphological data? Palaeontology 66(6):e12679.

Barido-Sottani J., Van Tiel N.M.A., Hopkins M.J., Wright D.F., Stadler T., Warnock R.C.M. 2020. Ignoring fossil age uncertainty leads to inaccurate topology and divergence time estimates in time calibrated tree inference. Front. Ecol. Evol. 8:183.

Beck R.M.D., Lee M.S.Y. 2014. Ancient dates or accelerated rates? Morphological clocks and the antiquity of placental mammals. Proc. R Soc. B. 281(1793):20141278.

Bell M.A., Lloyd G.T. 2015. strap: an R package for plotting phylogenies against stratigraphy and assessing their stratigraphic congruence. Palaeontology. 58(2):379–389.

Benton M.J., Ayala F.J. 2003. Dating the tree of life. Science. 300:1698–1700.

Bortolussi N., Durand E., Blum M., François O. 2006. apTreeshape: statistical analysis of phylogenetic tree shape. Bioinformatics 22(3):363–364.

Bromham L., Penny D. 2003. The modern molecular clock. Nat. Rev. Genet. 4(3):216–224.

Bronstein O., Kroh A., Haring E. 2018. Mind the gap! The mitochondrial control region and its power as a phylogenetic marker in echinoids. BMC Evol. Biol. 18(1):1–15.

Caetano D.S., Quental T.B. 2023. How important is budding speciation for comparative studies? Syst. Biol. 72(6):1443–1453.

Camacho C., Coulouris G., Avagyan V., Ma N., Papadopoulos J., Bealer K., Madden T.L. 2009. BLAST+: architecture and applications. BMC Bioinf. 10(1):1–9.

Capella-Gutiérrez S., Silla-Martínez J.M., Gabaldón T. 2009. trimAl: a tool for automated alignment trimming in large-scale phylogenetic analyses. Bioinformatics. 25(15):1972–1973.

Casali D. de melo, Dos Santos J.E., Miranda F.R., Santos F.R., Perini F.A. 2020. Total-evidence phylogeny and divergence times of *Vermilingua* (Mammalia: Pilosa). Syst. Biodivers. 18(3):216–227.

Casali D.M., Boscaini A., Gaudin T.J., Perini F.A. 2022. Reassessing the phylogeny and divergence times of sloths (Mammalia: Pilosa: Folivora), exploring alternative morphological partitioning and dating models. Zool. J. Linn. Soc. 196(4):1505–1551.

Chernomor O., Von Haeseler A., Minh B.Q. 2016. Terrace aware data structure for phylogenomic inference from supermatrices. Syst. Biol. 65(6):997–1008.

Clark H.L. 1938. Echinoderms from Australia: an account of collections made in 1929 and 1932. Mem. Mus. Comp. Zoöol. Harvard Coll. 55:1–597.
Clarke J.A., Middleton K.M. 2008. Mosaicism, modules, and the evolution of birds: results from a Bayesian approach to the study of morphological evolution using discrete character data. Syst. Biol. 57(2):185–201.
Coiro M., Allio R., Mazet N., Seyfullah L.J., Condamine F.L. 2023. Reconciling fossils with phylogenies reveals the origin and macroevolutionary processes explaining the global cycad biodiversity. New Phytol. 240(4):1616–1635.
Cracraft J., Donoghue M.J. 2004. Assembling the tree of life. New York: Oxford University Press.
Crisp M.D., Hardy N.B., Cook L.G. 2014. Clock model makes a large difference to age estimates of long-stemmed clades with no internal calibration: a test using Australian grasstrees. BMC Evol. Biol. 14(1):1–17.
Crouch N.M.A., Edie S.M., Collins K.S., Bieler R., Jablonski D. 2021. Calibrating phylogenies assuming bifurcation or budding alters inferred macroevolutionary dynamics in a densely sampled phylogeny of bivalve families. Proc. R Soc. B. 288(1964):20212178.
Darwin C. 1859. On the origin of species by means of natural selection. London: John Murray.
Deline B., Thompson J.R., Smith N.S., Zamora S., Rahman I.A., Sheffield S.L., Ausich W.I., Kammer T.W., Sumrall C.D. 2020. Evolution and development at the origin of a phylum. Curr. Biol. 30(9):1672–1679.e3.
Delle Chiaje S. 1824. Descrizione zoologica ed anatomica di alcune specie di Oloturie. Napoli: Memorie su la storia e notomia degli animali senza vertebre del Regno di Napoli. p. 77–116.
Dembo M., Radovčić D., Garvin H.M., Laird M.F., Schroeder L., Scott J.E., Brophy J., Ackermann R.R., Musiba C.M., de Ruiter D.J. 2016. The evolutionary relationships and age of Homo naledi: an assessment using dated Bayesian phylogenetic methods. J. Hum. Evol. 97:17–26.
Dos Reis M., Gunnell G.F., Barba-Montoya J., Wilkins A., Yang Z., Yoder A.D. 2018. Using phylogenomic data to explore the effects of relaxed clocks and calibration strategies on divergence time estimation: primates as a test case. Syst. Biol. 67(4):594–615.
Drummond A.J., Ho S.Y.W., Phillips M.J., Rambaut A. 2006. Relaxed phylogenetics and dating with confidence. PLoS Biol. 4(5):e88.
Drummond A.J., Rambaut A. 2007. BEAST: Bayesian evolutionary analysis by sampling trees. BMC Evol. Biol. 7(1):1–8.
Duchêne S., Molak M., Ho S.Y.W. 2014. ClockstaR: choosing the number of relaxed-clock models in molecular phylogenetic analysis. Bioinformatics. 30:1017–1019.
Durham J.W., Melville R.V. 1957. A classification of echinoids. J. Paleontol. 31: 242–272.
Erkenbrack E.M., Thompson J.R. 2019. Cell type phylogenetics informs the evolutionary origin of echinoderm larval skeletogenic cell identity. Commun. Biol. 2(1):160.
Fau M., Villier L. 2023. Mesozoic stem-group zoroasterid sea stars imply a delayed radiation of the crown group and adaptation to the deep seas. J. Syst. Paleontol. 21(1):2243268.
Faurby S., Silvestro D., Werdelin L., Antonelli A. 2024. Reliable biogeography requires fossils: insights from a new species-level phylogeny of extinct and living carnivores. Proc. R Soc. B. 291(2028):20240473.
FitzJohn R.G., Maddison W.P., Otto S.P. 2009. Estimating trait-dependent speciation and extinction rates from incompletely resolved phylogenies. Syst. Biol. 58(6):595–611.
Flores J.R., Bippus A.C., de Ullivarri C.F., Suárez G.M., Hyvönen J., Tomescu A.M.F. 2023. Dating the evolution of the complex thalloid liverworts (Marchantiopsida): total-evidence dating analysis supports a Late Silurian-Early Devonian origin and post-Mesozoic morphological stasis. New Phytol. 240(5):2137–2150.
Foote M. 1996. On the probability of ancestors in the fossil record. Paleobiology 22(2):141–151.
Gainett G., Klementz B.C., Blaszczyk P., Setton E.V.W., Murayama G.P., Willemart R., Gavish-Regev E., Sharma P.P. 2024. Vestigial organs alter fossil placements in an ancient group of terrestrial chelicerates. Curr. Biol. 34(6):1258–1270.e5.
Gavryushkina A., Heath T.A., Ksepka D.T., Stadler T., Welch D., Drummond A.J. 2017. Bayesian total-evidence dating reveals the recent crown radiation of penguins. Syst. Biol. 66:57–73.
Gavryushkina A., Welch D., Stadler T., Drummond A.J. 2014. Bayesian inference of sampled ancestor trees for epidemiology and fossil calibration. PLoS Comput. Biol. 10(12):e1003919.
Gillespie J.H. 1984. The molecular clock may be an episodic clock. Proc. Natl Acad. Sci. USA. 81(24):8009–8013.
Goloboff P.A. 1993. Estimating character weights during tree search. Cladistics. 9(1):83–91.
Goloboff P.A., Catalano S.A. 2016. TNT version 1.5, including a full implementation of phylogenetic morphometrics. Cladistics. 32(3):221–238.
Graur D., Martin W. 2004. Reading the entrails of chickens: molecular timescales of evolution and the illusion of precision. Trends Genet. 20(2):80–86.
Groom T.T. 1887. On some new features in *Pelanechinus corallinus*. Quart. J. Geol. Soc. London. 43(1-4):703–714.
Gustafson G.T., Prokin A.A., Bukontaite R., Bergsten J., Miller K.B. 2017. Tip-dated phylogeny of whirligig beetles reveals ancient lineage surviving on Sci. Rep. 7(1):8619.
Harvey P.H., May R.M., Nee S. 1994. Phylogenies without fossils. Evolution. 48:523–529.
Hawkins H.L. 1920. Morphological studies on the Echinoidea Holectypoida and their allies: X. On Apatopygus gen. nov. and the affinities of some recent Nucleolitoida and Cassiduloida. Geol. Mag. 57(9):393–401.
Heath T.A., Huelsenbeck J.P., Stadler T. 2014. The fossilized birth–death process for coherent calibration of divergence-time estimates. Proc. Natl Acad. Sci. USA 111(29):E2957–E2966.
Hedges S.B., Kumar S. 2004. Precision of molecular time estimates. Trends Genet. 20(5):242–247.
Hillis D.M., Heath T.A., John K.S. 2005. Analysis and visualization of tree space. Syst. Biol. 54(3):471–482.
Ho S.Y.W.editor. 2020. The molecular clock and evolutionary rates across the tree of life. The molecular evolutionary clock: theory and practice. Cham: Springer. p. 3–23.
Ho S.Y.W., Phillips M.J. 2009. Accounting for calibration uncertainty in phylogenetic estimation of evolutionary divergence times. Syst. Biol. 58(3):367–380.
Ho W.-C., Ohya Y., Zhang J. 2017. Testing the neutral hypothesis of phenotypic evolution. Proc. Natl Acad. Sci. USA. 114(46):12219–12224.
Höhna S., Stadler T., Ronquist F., Britton T. 2011. Inferring speciation and extinction rates under different sampling schemes. Mol. Biol. Evol. 28:2577–2589.
Holmes F.C. 1999. Australian tertiary Apatopygidae (Echinoidea). Proc. R. Soc. Vic. 111:51–70.
Hopkins M.J., Smith A.B. 2015. Dynamic evolutionary change in post-Paleozoic echinoids and the importance of scale when interpreting changes in rates of evolution. Proc. Natl Acad. Sci. USA. 112(12):3758–3763.
Hunt G., Slater G. 2016. Integrating paleontological and phylogenetic approaches to macroevolution. Annu. Rev. Ecol. Evol. Syst. 47(1):189–213.
Kalyaanamoorthy S., Minh B.Q., Wong T.K.F., Von Haeseler A., Jermiin L.S. 2017. ModelFinder: fast model selection for accurate phylogenetic estimates. Nat. Methods. 14(6):587–589.
Katoh K., Standley D.M. 2013. MAFFT multiple sequence alignment software version 7: improvements in performance and usability. Mol. Biol. Evol. 30(4):772–780.
Khakurel B., Grigsby C., Tran T.D., Zariwala J., Höhna S., Wright A.M. 2024. The fundamental role of character coding in Bayesian morphological phylogenetics. Syst. Biol. 73: 861–871.
Kier P.M. 1962. Revision of the cassiduloid echinoids. Washington D.C.: Smithsonian Miscellaneous Collections.
Kier P.M. 1966. Cassiduloids. In: Moore R.C., editor. Treatise on invertebrate paleontology. Part U, Echinodermata 3, Vol. 2. Lawrence, KS: Univesity of Kansas Press. p.U492–U523.

Kimura M. 1969. The rate of molecular evolution considered from the standpoint of population genetics. Proc. Natl Acad. Sci. USA 63(4):1181–1188.
King B. 2021. Bayesian tip-dated phylogenetics in paleontology: topological effects and stratigraphic fit. Syst. Biol. 70(2):283–294.
King B., Qiao T., Lee M.S.Y., Zhu M., Long J.A. 2017. Bayesian morphological clock methods resurrect placoderm monophyly and reveal rapid early evolution in jawed vertebrates. Syst. Biol. 66:499–516.
Klopfstein S., Ryer R., Coiro M., Spasojevic T. 2019. Mismatch of the morphology model is mostly unproblematic in total-evidence dating: insights from an extensive simulation study. bioRxiv. https://doi.org/10.1101/679084
Kroh A. 2020. Phylogeny and classification of echinoids. Dev. Aquacult. Fish. Sci. 43:1–17.
Kroh A., Mooi R. 2024. World Echinoidea Database. https://www.marinespecies.org/echinoidea. Accessed July 2021
Kroh A., Smith A.B. 2010. The phylogeny and classification of post-Palaeozoic echinoids. J. Syst. Paleontol. 8(2):147–212.
Kumar S. 2005. Molecular clocks: four decades of evolution. Nat. Rev. Genet. 6(8):654–662.
Lam A.R., Sheffield S.L., Matzke N.J. 2021. Estimating dispersal and evolutionary dynamics in diploporan blastozoans (Echinodermata) across the great Ordovician biodiversification event. Paleobiology. 47(2):198–220.
Lanfear R., Frandsen P.B., Wright A.M., Senfeld T., Calcott B. 2017. PartitionFinder 2: new methods for selecting partitioned models of evolution for molecular and morphological phylogenetic analyses. Mol. Biol. Evol. 34:772–773.
Lartillot N., Phillips M.J., Ronquist F. 2016. A mixed relaxed clock model. Phil. Trans. R. Soc. B. 371(1699):20150132.
Lee H., Lee K.-S., Hsu C.-H., Lee C.-W., Li C.-E., Wang J.-K., Tseng C., Chen W.-J., Horng C.-C., Ford C.T. 2023. Phylogeny, ancestral ranges and reclassification of sand dollars. Sci. Rep. 13(1):10199.
Lee M.S.Y. 2016. Multiple morphological clocks and total-evidence tip-dating in mammals. Biol. Lett. 12(7):20160033.
Lee M.S.Y., Cau A., Naish D., Dyke G.J. 2014. Morphological clocks in paleontology, and a mid-Cretaceous origin of crown Aves. Syst. Biol. 63(3):442–449.
Lee M.S.Y., Palci A. 2015. Morphological phylogenetics in the genomic age. Curr. Biol. 25(19):R922–R929.
Lee M.S.Y., Worthy T.H. 2012. Likelihood reinstates *Archaeopteryx* as a primitive bird. Biol. Lett. 8(2):299–303.
Lee M.S.Y., Yates A.M. 2018. Tip-dating and homoplasy: reconciling the shallow molecular divergences of modern gharials with their long fossil record. Proc. R Soc. B. 285(1881):20181071.
Lepage T., Bryant D., Philippe H., Lartillot N. 2007. A general comparison of relaxed molecular clock models. Mol. Biol. Evol. 24(12):2669–2680.
Lepeco A., Melo G.A.R. 2024. Revisiting the phylogeny of the scolebythid wasps (Hymenoptera: Aculeata) through Bayesian model evaluation and parsimony, with description of a new fossil family of Chrysidoidea. Zool. J. Linn. Soc. 201(1):57–85.
Lewis P.O. 2001. A likelihood approach to estimating phylogeny from discrete morphological character data. Syst. Biol. 50(6):913–925.
Littlewood D.T.J., Smith A.B. 1995. A combined morphological and molecular phylogeny for sea urchins (Echinoidea: Echinodermata). Philos. Trans. R. Soc. London. B Biol. Sci. 347:213–234.
López-Antoñanzas R., Mitchell J., Simões T.R., Condamine F.L., Aguilée R., Peláez-Campomanes P., Renaud S., Rolland J., Donoghue P.C.J. 2022. Integrative phylogenetics: tools for palaeontologists to explore the Tree of Life. Biology (Basel). 11:1185.
Luo A., Duchêne D.A., Zhang C., Zhu C.-D., Ho S.Y.W. 2020. A simulation-based evaluation of tip-dating under the fossilized birth–death process. Syst. Biol. 69(2):325–344.
Maddison D.R., Schulz K.-S., Maddison W.P. 2007. The tree of life web project. Zootaxa. 1668(1):19–40.
Matschiner M. 2019. Selective sampling of species and fossils influences age estimates under the fossilized birth–death model. Front. Genet. 10:1064.
May M.R., Contreras D.L., Sundue M.A., Nagalingum N.S., Looy C. V, Rothfels C.J. 2021. Inferring the total-evidence timescale of marattialean fern evolution in the face of model sensitivity. Syst. Biol. 70(6):1232–1255.
Mayr E. 1963. The taxonomic evaluation of early hominids. In: Washburn S., editor. Classification and evolution. Chicago, IL: Aldine. p. 332–346.
Milne Edwards H. 1836. Les zoophytes. In: Cuvier G., editor. Le règne animal distribué d'après son organisation, pour servir de base à l'histoire naturelle des animaux, et d'introduction à l'anatomie comparée, Ed. 3, Tome 11 [Atlas]. Paris: Chez De´terville.
Minh B.Q., Schmidt H.A., Chernomor O., Schrempf D., Woodhams M.D., Von Haeseler A., Lanfear R. 2020. IQ-TREE 2: new models and efficient methods for phylogenetic inference in the genomic era. Mol. Biol. Evol. 37(5):1530–1534.
Minin K. V, Mironov A.N., Petrov N.B., Vladychenskaya I.P. 2024. Evolutionary and biogeographic patterns in the deep-sea echinoid families Pourtalesiidae Agassiz 1881 and Ceratophysidae fam. nov. (Echinoidea). Zool. J. Linn. Soc. 202(4):zlae034.
Mongiardino Koch N. 2021a. Exploring adaptive landscapes across deep time: a case study using echinoid body size. Evolution. 75:1567–1581.
Mongiardino Koch N. 2021b. Phylogenomic subsampling and the search for phylogenetically reliable loci. Mol. Biol. Evol. 38(9):4025–4038.
Mongiardino Koch N., Coppard S.E., Lessios H.A., Briggs D.E.G., Mooi R., Rouse G.W. 2018. A phylogenomic resolution of the sea urchin tree of life. BMC Evol. Biol. 18(1):1–18.
Mongiardino Koch N., Garwood R.J., Parry L.A. 2023. Inaccurate fossil placement does not compromise tip-dated divergence times. Palaeontology. 66(6):e12680.
Mongiardino Koch N., Milla Carmona P. 2024. Chronospaces: an R package for the statistical exploration of divergence times promotes the assessment of methodological sensitivity. Methods Ecol. Evol. 15(10):1822–1833.
Mongiardino Koch N., Thompson J.R. 2021. A total-evidence dated phylogeny of Echinoidea combining phylogenomic and paleontological data. Syst. Biol. 70(3):421–439.
Mongiardino Koch N., Thompson J.R., Hiley A.S., McCowin M.F., Armstrong A.F., Coppard S.E., Aguilera F., Bronstein O., Kroh A., Mooi R., Rouse G.W. 2022. Phylogenomic analyses of echinoid diversification prompt a re-evaluation of their fossil record. eLife. 11:e72460.
Mooi R. 1990. Living Cassiduloids (Echinodermata, Echinoidea)—a key and annotated list. Proc. Biol. Soc. Wash. 10363:85.
Morgan G.J. 1998. Emile Zuckerkandl, Linus Pauling, and the molecular evolutionary clock, 1959-1965. J. Hist. Biol. 31(2):155–178.
Mortensen T. 1903. *Lissodiadema*: nouveau genre de diadematides. Rev. Suisse Zool. 11:393–398.
Mortensen T. 1948. A monograph of the Echinoidea. IV, 1 Holectypoida, Cassiduloida. Copenhagen: C. A. Reitzel.
Mulvey L.P.A., May M.R., Brown J.M., Hoehna S., Wright A.M., Warnock R.C.M. 2025. Assessing the Adequacy of Morphological Models Using Posterior Predictive Simulations. Syst. Biol. 74(1):34–52.
Mulvey L.P.A., Nikolic M.C., Allen B.J., Heath T.A., Warnock R.C.M. 2025. From fossils to phylogenies: exploring the integration of paleontological data into Bayesian phylogenetic inference. Paleobiology. 51(1): 214–236.
Oksanen J., Simpson G., Blanchet F., Kindt R., Legendre P., Minchin P., O'Hara R., Solymos P., Stevens M., Szoecs E., Wagner H., Barbour M., Bedward M., Bolker B., Borcard D., Carvalho G., Chirico M., De Caceres M., Durand S., Evangelista H., FitzJohn R., Friendly M., Furneaux B., Hannigan G., Hill M., Lahti L., McGlinn D., Ouellette M., Ribeiro Cunha E., Smith T., Stier A., Ter Braak C., Weedon J. 2024. vegan: community Ecology Package. R package version 2.6-8.
O'Reilly J.E., Donoghue P.C.J. 2020. The effect of fossil sampling on the estimation of divergence times with the fossilized birth–death process. Syst. Biol. 69:124–138.
O'Reilly J.E., Dos Reis M., Donoghue P.C.J. 2015. Dating tips for divergence-time estimation. Trends Genet. 31:637–650.

Paradis E., Schliep K. 2019. ape 5.0: an environment for modern phylogenetics and evolutionary analyses in R. Bioinformatics. 35(3):526–528.
Parins-Fukuchi C.T., Saulsbury J.G. 2025. The consequences of budding speciation on trees. Syst. Biol. 74: 499–510.
Perseke M., Bernhard D., Fritzsch G., Brümmer F., Stadler P.F., Schlegel M. 2010. Mitochondrial genome evolution in Ophiuroidea, Echinoidea, and Holothuroidea: insights in phylogenetic relationships of Echinodermata. Mol. Phylogenet. Evol. 56(1):201–211.
Pett W., Heath T.A. 2020. Inferring the timescale of phylogenetic trees from fossil data. In: Scornavacca C., Delsuc F., Galtier N., editors Phylogenetics in the genomic era. Hyper Articles en Ligne (HAL). p.5.1:1–5.1:18.
Philip G.M. 1965. Classification of echinoids. J. Paleontol. 39: 45–62.
Philippi R.A. 1845. Beschreibung einiger neuer Echinodermen nebst kritischen Bemerckungen über einige weniger bekannte Arten. Archiv für Naturgeschichte. 11:344–359.
Picciani N., Kerlin J.R., Sierra N., Swafford A.J.M., Ramirez M.D., Roberts N.G., Cannon J.T., Daly M., Oakley T.H. 2018. Prolific origination of eyes in Cnidaria with co-option of non-visual opsins. Curr. Biol. 28(15):2413–2419.e4.
Pol D., Norell M.A. 2001. Comments on the Manhattan stratigraphic measure. Cladistics 17(3):285–289.
Pyron R.A. 2011. Divergence time estimation using fossils as terminal taxa and the origins of *Lissamphibia*. Syst. Biol. 60(4):466–481.
Pyron R.A. 2015. Post-molecular systematics and the future of phylogenetics. Trends Ecol. Evol. 30(7):384–389.
Pyron R.A. 2017. Novel approaches for phylogenetic inference from morphological data and total-evidence dating in squamate reptiles (lizards, snakes, and amphisbaenians). Syst. Biol. 66:38–56.
R Core Team. 2024. R: a language and environment for statistical computing. Vienna: R Foundation for Statistical Computing.
Rahman I.A., Thompson J.R., Briggs D.E.G., Siveter D.J., Siveter D.J., Sutton M.D. 2019. A new ophiocistioid with soft-tissue preservation from the Silurian Herefordshire Lagerstätte, and the evolution of the holothurian body plan. Proc. R Soc. B. 286(1900):20182792.
Rambaut A., Bromham L. 1998. Estimating divergence dates from molecular sequences. Mol. Biol. Evol. 15(4):442–448.
Rambaut A., Drummond A.J., Xie D., Baele G., Suchard M.A. 2018. Posterior summarization in Bayesian phylogenetics using Tracer 1.7. Syst. Biol. 67(5):901–904.
Rieseberg L.H., Widmer A., Arntz A.M., Burke J.M. 2002. Directional selection is the primary cause of phenotypic diversification. Proc. Natl Acad. Sci. USA. 99(19):12242–12245.
Ronquist F., Klopfstein S., Vilhelmsen L., Schulmeister S., Murray D.L., Rasnitsyn A.P. 2012a. A total-evidence approach to dating with fossils, applied to the early radiation of the Hymenoptera. Syst. Biol. 61(6):973–999.
Ronquist F., Lartillot N., Phillips M.J. 2016. Closing the gap between rocks and clocks using total-evidence dating. Phil. Trans. R. Soc. B. 371(1699):20150136.
Ronquist F., Teslenko M., Van Der Mark P., Ayres D.L., Darling A., Höhna S., Larget B., Liu L., Suchard M.A., Huelsenbeck J.P. 2012b. MrBayes 3.2: efficient Bayesian phylogenetic inference and model choice across a large model space. Syst. Biol. 61(3):539–542.
Rosa B.B., Melo G.A.R., Barbeitos M.S. 2019. Homoplasy-based partitioning outperforms alternatives in Bayesian analysis of discrete morphological data. Syst. Biol. 68(4):657–671.
Sand A., Holt M.K., Johansen J., Brodal G.S., Mailund T., Pedersen C.N.S. 2014. tqDist: a library for computing the quartet and triplet distances between binary or general trees. Bioinformatics. 30(14):2079–2080.
Sanderson M.J. 1997. A nonparametric approach to estimating divergence times in the absence of rate constancy. Mol. Biol. Evol. 14(12):1218–1231.
Saucède T., Néraudeau D. 2006. An "Elvis" echinoid, Nucleopygus (Jolyclypus) jolyi, from the Cenomanian of France: phylogenetic analysis, sexual dimorphism and neotype designation. Cretac Res. 27:542–554.
Saulsbury J.G., Baumiller T.K. 2023. Dispersals from the West Tethys as the source of the Indo-West Pacific diversity hotspot in comatulid crinoids. Paleobiology. 49(1):39–52.
Schliep K.P. 2011. phangorn: phylogenetic analysis in R. Bioinformatics. 27(4):592–593.
Sharma P.P., Giribet G. 2014. A revised dated phylogeny of the arachnid order Opiliones. Front. Genet. 5:255.
Simões T.R., Caldwell M.W., Pierce S.E. 2020a. Sphenodontian phylogeny and the impact of model choice in Bayesian morphological clock estimates of divergence times and evolutionary rates. BMC Biol. 18:1–30.
Simões T.R., Greifer N., Barido-Sottani J., Pierce S.E. 2023a. EvoPhylo: an R package for pre-and postprocessing of morphological data from relaxed clock Bayesian phylogenetics. Methods Ecol. Evol. 14:1981–1993.
Simões T.R., Vernygora O., Caldwell M.W., Pierce S.E. 2020b. Megaevolutionary dynamics and the timing of evolutionary innovation in reptiles. Nat. Commun. 11:3322.
Simões T.R., Vernygora O. V., de Medeiros B.A.S., Wright A.M. 2023b. Handling logical character dependency in phylogenetic inference: extensive performance testing of assumptions and solutions using simulated and empirical data. Syst. Biol. 72:662–680.
Simpson G.G. 1965. Organisms and molecules in evolution. In: Peeters H., editor. Protides of the biological fluids. Amsterdam: Elsevier. p. 29–35.
Smith A.B. 1981. Implications of lantern morphology for the phylogeny of post-Palaeozoic echinoids.Palaeontology. 24(4):779–801.
Smith A.B. 1984. Echinoid palaeobiology. London: George Allen & Unwin.
Smith A.B. 1990. Echinoid evolution from the Triassic to the Lower Jurassic Cahiers Université Catholique de Lyon, série Sciences. 3:79–117.
Smith A.B. 1994. Triassic echinoids from Peru. pala. 233(1-6):177–202.
Smith A.B. 2007. Intrinsic versus extrinsic biases in the fossil record: contrasting the fossil record of echinoids in the Triassic and early Jurassic using sampling data, phylogenetic analysis, and molecular clocks. Paleobiology 33(2):310–323.
Smith A.B. 2015. British Jurassic Regular Echinoids. Part 1, Introduction, Cidaroida, Echinothurioida, Aspidodiadematoida and Pedinoida. Monogr. Palaeontogr. Soc. 169(644):1–67.
Smith A.B., Hollingworth N.T.J. 1990. Tooth structure and phylogeny of the Upper Permian echinoid *Miocidaris keyserlingi*. Proc. Yorks. Geol. Soc. 48(1):47–60.
Smith A.B., Pisani D., Mackenzie-Dodds J.A., Stockley B., Webster B.L., Littlewood D.T.J. 2006. Testing the molecular clock: molecular and paleontological estimates of divergence times in the Echinoidea (Echinodermata). Mol. Biol. Evol. 23(10):1832–1851.
Smith M.R. 2019. Quartet: comparison of phylogenetic trees using quartet and bipartition measures. Comprehensive R Archive Network. 10.
Smith M.R. 2022. Robust analysis of phylogenetic tree space. Syst. Biol. 71(5):1255–1270.
Souto C., Mooi R., Martins L., Menegola C., Marshall C.R. 2019. Homoplasy and extinction: the phylogeny of cassidulid echinoids (Echinodermata). Zool. J. Linn. Soc. 187(3):622–660.
Suter S.J. 1994. Cladistic analysis of cassiduloid echinoids: trying to see the phylogeny for the trees. Biol. J. Linn. Soc. 53(1):31–72.
Tao Q., Tamura K., U. Battistuzzi F., Kumar S. 2019. A machine learning method for detecting autocorrelation of evolutionary rates in large phylogenies. Mol. Biol. Evol. 36(4):811–824.
Tarasov S., Genier F. 2015. Innovative Bayesian and parsimony phylogeny of dung beetles (Coleoptera, Scarabaeidae, Scarabaeinae) enhanced by ontology-based partitioning of morphological characters. PLoS One 10(3):e0116671.
Tejada J. V, Antoine P.-O., Münch P., Billet G., Hautier L., Delsuc F., Condamine F.L. 2024. Bayesian total-evidence dating revisits sloth phylogeny and biogeography: a cautionary tale on morphological clock analyses. Syst. Biol. 73(1):125–139.
Thompson J.R., Erkenbrack E.M., Hinman V.F., McCauley B.S., Petsios E., Bottjer D.J. 2017. Paleogenomics of echinoids reveals an ancient

origin for the double-negative specification of micromeres in sea urchins. Proc. Natl Acad. Sci. USA. 114(23):5870–5877.
Thompson J.R., Mirantsev G. V, Petsios E., Bottjer D.J. 2020. Phylogenetic analysis of the Archaeocidaridae and Palaeozoic Miocidaridae (Echinodermata, Echinoidea) and the origin of crown group echinoids. Pap. Palaeontol. 6(2):217–249.
Thompson J.R., Petsios E., Davidson E.H., Erkenbrack E.M., Gao F., Bottjer D.J. 2015. Reorganization of sea urchin gene regulatory networks at least 268 million years ago as revealed by oldest fossil cidaroid echinoid. Sci. Rep. 5(1):15541.
Thompson J.R., Posenato R., Bottjer D.J., Petsios E. 2019. Echinoids from the Tesero Member (Werfen Formation) of the Dolomites (Italy): implications for extinction and survival of echinoids in the aftermath of the end-Permian mass extinction. PeerJ. 7:e7361.
Thomson C.T.W. 1872. On the Echinidea of the "Porcupine" deep-sea dredging-expeditions. Proc. R. Soc. London. 20:491–497.
Thorne J.L., Kishino H. 2002. Divergence time and evolutionary rate estimation with multilocus data. Syst. Biol. 51(5):689–702.
Thorne J.L., Kishino H., Painter I.S. 1998. Estimating the rate of evolution of the rate of molecular evolution. Mol. Biol. Evol. 15(12):1647–1657.
Thuy B., Eriksson M.E., Kutscher M., Lindgren J., Numberger-Thuy L.D., Wright D.F. 2022. Miniaturization during a Silurian environmental crisis generated the modern brittle star body plan. Commun. Biol. 5(1):14.
Thuy B., Stöhr S. 2016. A new morphological phylogeny of the Ophiuroidea (Echinodermata) accords with molecular evidence and renders microfossils accessible for cladistics. PLoS One. 11(5):e0156140.
Troyer E.M., Betancur-R R., Hughes L.C., Westneat M., Carnevale G., White W.T., Pogonoski J.J., Tyler J.C., Baldwin C.C., Ortí G. 2022. The impact of paleoclimatic changes on body size evolution in marine fishes. Proc. Natl Acad. Sci. USA. 119(29):e2122486119.
Turner A.H., Pritchard A.C., Matzke N.J. 2017. Empirical and Bayesian approaches to fossil-only divergence times: a study across three reptile clades. PLoS One. 12(2):e0169885.
Van Dongen S. 2000. Graph clustering by flow simulation. PhD thesis, University of Utrecht.
Warnock R.C.M., Wright A.M. 2020. Understanding the tripartite approach to Bayesian divergence time estimation. Elements of Paleontology. Cambridge: Cambridge University Press.
Warren D.L., Geneva A.J., Lanfear R. 2017. RWTY (R we there yet): an R package for examining convergence of Bayesian phylogenetic analyses. Mol. Biol. Evol. 34:1016–1020.
Wickham H., Averick M., Bryan J., Chang W., McGowan L.D., François R., Grolemund G., Hayes A., Henry L., Hester J. 2019. Welcome to the Tidyverse. J. Open Source Softw. 4(43):1686.
WoRMS Editorial Board. 2024. World Register of Marine Species. https://www.marinespecies.org. Accessed on July 2021.
Wright A.M., Bapst D.W., Barido-Sottani J., Warnock R.C.M. 2022. Integrating fossil observations into phylogenetics using the fossilized birth–death model. Annu. Rev. Ecol. Evol. Syst. 53(1):251–273.
Wright A.M., Hillis D.M. 2014. Bayesian analysis using a simple likelihood model outperforms parsimony for estimation of phylogeny from discrete morphological data. PLoS One. 9(10):e109210.
Wright A.M., Lloyd G.T., Hillis D.M. 2016. Modeling character change heterogeneity in phylogenetic analyses of morphology through the use of priors. Syst. Biol. 65(4):602–611.
Wright A.M., Wagner P.J., Wright D.F. 2021. Testing character evolution models in phylogenetic paleobiology: a case study with Cambrian echinoderms. Elements in Paleontology. Cambridge: Cambridge University Press.
Wright A.M., Wynd B.M. 2024. Modeling of rate heterogeneity in datasets compiled for use with parsimony. bioRxiv. 2024.06.26.600858. https://doi.org/10.1101/2024.06.26.600858.
Wright D.F. 2017. Bayesian estimation of fossil phylogenies and the evolution of early to middle Paleozoic crinoids (Echinodermata). J. Paleontol. 91(4):799–814.
Yang Y., Smith S.A. 2014. Orthology inference in nonmodel organisms using transcriptomes and low-coverage genomes: improving accuracy and matrix occupancy for phylogenomics. Mol. Biol. Evol. 31(11):3081–3092.
Yang Z., Rannala B. 2006. Bayesian estimation of species divergence times under a molecular clock using multiple fossil calibrations with soft bounds. Mol. Biol. Evol. 23(1):212–226.
Yoder A.D., Yang Z. 2000. Estimation of primate speciation dates using local molecular clocks. Mol. Biol. Evol. 17(7):1081–1090.
Zhang C., Ronquist F., Stadler T. 2023. Skyline fossilized birth–death model is robust to violations of sampling assumptions in total-evidence dating. Syst. Biol. 72(6):1316–1336.
Zhang C., Stadler T., Klopfstein S., Heath T.A., Ronquist F. 2016. Total-evidence dating under the fossilized birth–death process. Syst. Biol. 65(2):228–249.
Zuckerkandl E. 1987. On the molecular evolutionary clock. J. Mol. Evol. 26(1-2):34–46.
Zuckerkandl E., Pauling L. 1962. Molecular disease, evolution and genic heterogeneity. In: Kasha M., Pullman B., editors. Horizons in biochemistry: Albert Szent-Gyorgyi dedicatory volume. New York: Academic Press. p. 189–225.
Zuckerkandl E., Pauling L. 1965. Evolutionary divergence and convergence in proteins.In: B., Vogel H. J. Vernon, editors. Evolving genes and proteins. Cambridge: Academic Press. p.97–166.

Syst. Biol. 75(1):135–155, 2026

https://doi.org/10.1093/sysbio/syaf055
Advance Access publication August 8, 2025